

REVIEW



Cite this: *Mater. Chem. Front.*,
2021, 5, 6693

Received 1st June 2021,
Accepted 12th July 2021

DOI: 10.1039/d1qm00808k

rsc.li/frontiers-materials

Clusterization-triggered emission (CTE): one for all, all for one

Peilong Liao,^a Jianbin Huang,^a Yun Yan *^a and Ben Zhong Tang*^b

One for all and all for one, hand in hand turns the light on. Clusterization-triggered emission (CTE) is a photophysical phenomenon that has attracted increased attention in recent years. Highly efficient luminescence based on through-space conjugation (TSC) can be obtained due to the clusterization of non-conventional chromophore-forming clusteroluminogens with extended electron delocalization and a rigid conformation. The CTE process makes it possible to generate highly efficient light emitters from a vast variety of non-conjugated molecules. It is anticipated that CTE may bring about a revolution in the design of advanced functional luminescent materials in the future. In this review, we systematically summarize the current status of CTE studies, aiming at analysing the future development trends in this field. The following issues are discussed: (1) TSC hypothesis and experimental confirmation; (2) characteristics of CTE, including concentration-enhanced luminescence, excitation wavelength-dependent emission, room temperature phosphorescence (RTP) and polarization-enhanced luminescence; (3) typical examples of CTE systems, including biomacromolecules, multicolor luminescent polymers and organic–inorganic hybrid materials; and (4) applications of the CTE effect, including optical anti-counterfeiting, white LED materials, bioimaging, and molecular sensing. We envisage that the supramolecular self-assembly of CTE systems will become an important direction in the field of CTE research.

^a Beijing National Laboratory for Molecular Sciences (BNLMS), College of Chemistry and Molecular Engineering, Peking University, Beijing 100871, China.

E-mail: yunyan@pku.edu.cn

^b Department of Chemistry, Shenzhen Institute of Aggregate Science and Technology, School of Science and Engineering, The Chinese University of Hong Kong, Shenzhen, Guangdong 518172, China. E-mail: tangbenz@cuhk.edu.cn

Introduction

Luminescence is a widely observed phenomenon occurring throughout nature in both abiotic and biological worlds, such as the night pearl in the tomb of the emperor, the signal lamp on the butt of a firefly and fluorescent fungi in rainforests. People cannot help being attracted to them and are constantly



Peilong Liao

Peilong Liao is a graduate student at Peking University, under the guidance of Yun Yan and Jianbin Huang. He obtained his bachelor's degree from the same university in 2017. His studies focus on clusteroluminogen electrostatic assemblies and their related applications.



Jianbin Huang

Jianbin Huang obtained his Bachelor's (1987), Master's (1990), and PhD (1993) degrees from Peking University. He was nominated as an Associate Professor in 1995, as a Full Professor in 2001, and was awarded "Out-standing Young Scientist of China" in 2004. His main research interests include the soft self-assembly of amphiphiles and one-dimensional nano-materials synthesized by using soft templates. He is currently the Senior Editor of *Soft Matter* and is also the

Board Editor of *Langmuir* and the *Journal of Colloid and Interface Science*.

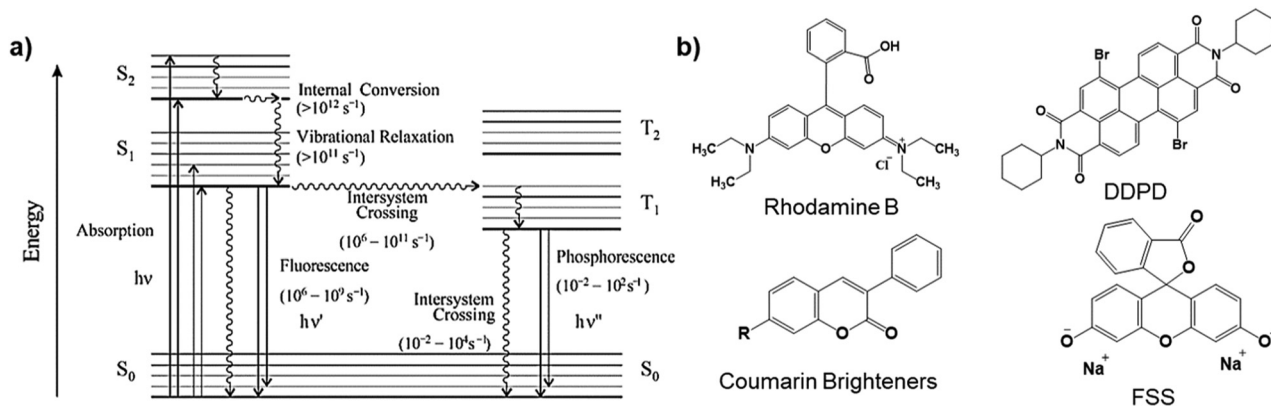


Fig. 1 (a) A typical Jablonski diagram. (b) Structures of typical traditional organic fluorescent molecules.

trying to understand the mechanisms behind all kinds of luminescence. In addition, breakthroughs in the understanding and applications of light-emitting processes have opened new avenues to scientific advancements and societal developments. The most famous example is the study of green fluorescent protein (GFP). The GFP gene was isolated from a fluorescent jellyfish family and was demonstrated to be scientifically significant for a wide variety of critical biological labelling/genetic studies. This work ultimately led to a Nobel Prize (2008) shared by Shimomura, Tsein¹ and Chalfie.²

So far, a deep and extensive understanding about the luminescence process for most fluorescence systems has been formed. Generally, this process requires specific atomic or molecular structures with delocalizable electrons that are suitable for participation in three critical mechanistic events to produce luminescence emission, namely (1) photon

absorption, (2) energy-induced, orbital electron excitation and (3) electron relaxation with energy loss to give luminescence emission. The entire process is illustrated by the Jablonski diagram (Fig. 1a). As such, suitable structures must possess photon absorption features sufficient to absorb and excite delocalizable electrons from the ground state (S_0) to an excited state (S_1), followed by relaxation/decay to the ground state (S_0) accompanied by lower energy luminescence emission. In traditional organic fluorescent materials, these structural criteria are found in broad categories of rigid, conjugated poly(aromatics), extended π systems or poly(unsaturated heterocyclic) systems containing high multiplicities of heteroatoms with unoccupied p-orbitals (Fig. 1b). These traditional luminophores usually function as individual, isolated molecular entities and exhibit concentration-dependent self-quenching effects.³



Yun Yan

Professor Yun Yan received her BS and PhD degrees from Northeast Normal University and Peking University, China, in 1997 and 2003, respectively. She conducted her postdoctoral work at Bayreuth University, Germany, and Wageningen University, the Netherlands, during 2004–2005, and 2005–2008, respectively. She joined Peking University in 2008, worked as a Visiting Scientist in Professor Ben Zhong Tang's group in HKUST (2016), and

was promoted to a Full Professor of Peking University in 2019. Her interests are in the methodology of molecular self-assembly. She is now serving as the General Secretary of Physical Chemistry of the Chinese Chemical Society, a member of the Association of Aggregation Induced Emission of the Chinese Chemical Society, an Advisory Board member of ACS Applied Materials & Interfaces, and as a Fellow of the International Association of Advanced Materials (FIAAM).



Ben Zhong Tang

Professor Ben Zhong Tang received his BS and PhD degrees from South China University of Technology and Kyoto University in 1982 and 1988, respectively. He conducted his postdoctoral work at the University of Toronto and worked as a Senior Scientist in Neos Co., Ltd in 1989–1994. He joined the Hong Kong University of Science & Technology in 1994 and was promoted to Chair Professor in 2008. In 2021, he joined Chinese Uni-

versity of Hong Kong (CUHK)-Shenzhen as the Dean of the School of Science and Engineering. He is serving as a News Contributor to Noteworthy Chemistry (ACS) and Editor-in-Chiefs of Materials Chemistry Frontiers (RSC), Polymer Chemistry Series (RSC), and Aggregate (Wiley).

In 1970, emission from a saturated amine named 1,4-diazabicyclo[2.2.2]octane (DABCO) excited at 250 nm in the gas phase at 25 °C was reported.⁴ This was the first reported example of non-traditional intrinsic blue luminescence that does not satisfy the accepted criteria of aromaticity or an extended π system required for traditional luminescence.

Since then, numerous reports have appeared describing inexplicable blue fluorescence in the absence of conventional luminophores. In 2001, a revolutionary concept referred to as aggregation-induced emission (AIE) was introduced by Tang *et al.*^{5,6} This described an uncommon luminogen system in which aggregation worked constructively, rather than destructively as in the conventional systems. Specifically, an AIE luminogen (AIEgen) shows weak or negligible emission in dilute solution but emits intensely in the aggregate or the solid state. Unlike conventional luminophores such as the disc-like planar perylene, AIEgens are usually propeller-shaped non-planar molecules.⁷ The restriction of intramolecular motions (RIM) is accepted as being

central to the AIE working mechanism. As shown in Fig. 2, the intramolecular motions (rotation and vibration) of AIEgens such as tetraphenylethene (TPE) and silole are rapid in dilute solution and the emission is quenched because of the high non-radiative decay rate (k_{nr}). However, because of the highly twisted conformation of AIEgens, both intermolecular π - π stacking and intramolecular motions are restricted in the aggregate or the solid state, which results in a suppressed k_{nr} . Therefore, the radiative decay rate (k_r) can now effectively compete with k_{nr} , leading to an enhanced emission quantum yield.⁸⁻¹⁰ As AIEgens often show unique advantages such as a high solid quantum yield, high photostability and anti-ACQ effects, they have been successfully applied in various fields such as OLEDs, stimuli-responsive sensing, bioimaging and theranostics.^{7,11-13}

Among the many studies on AIEgens, a series of molecules appear to be particularly special. These molecules show dim or no emission in dilute solution but a much enhanced emission in aggregates or in the solid state as typical AIE properties.

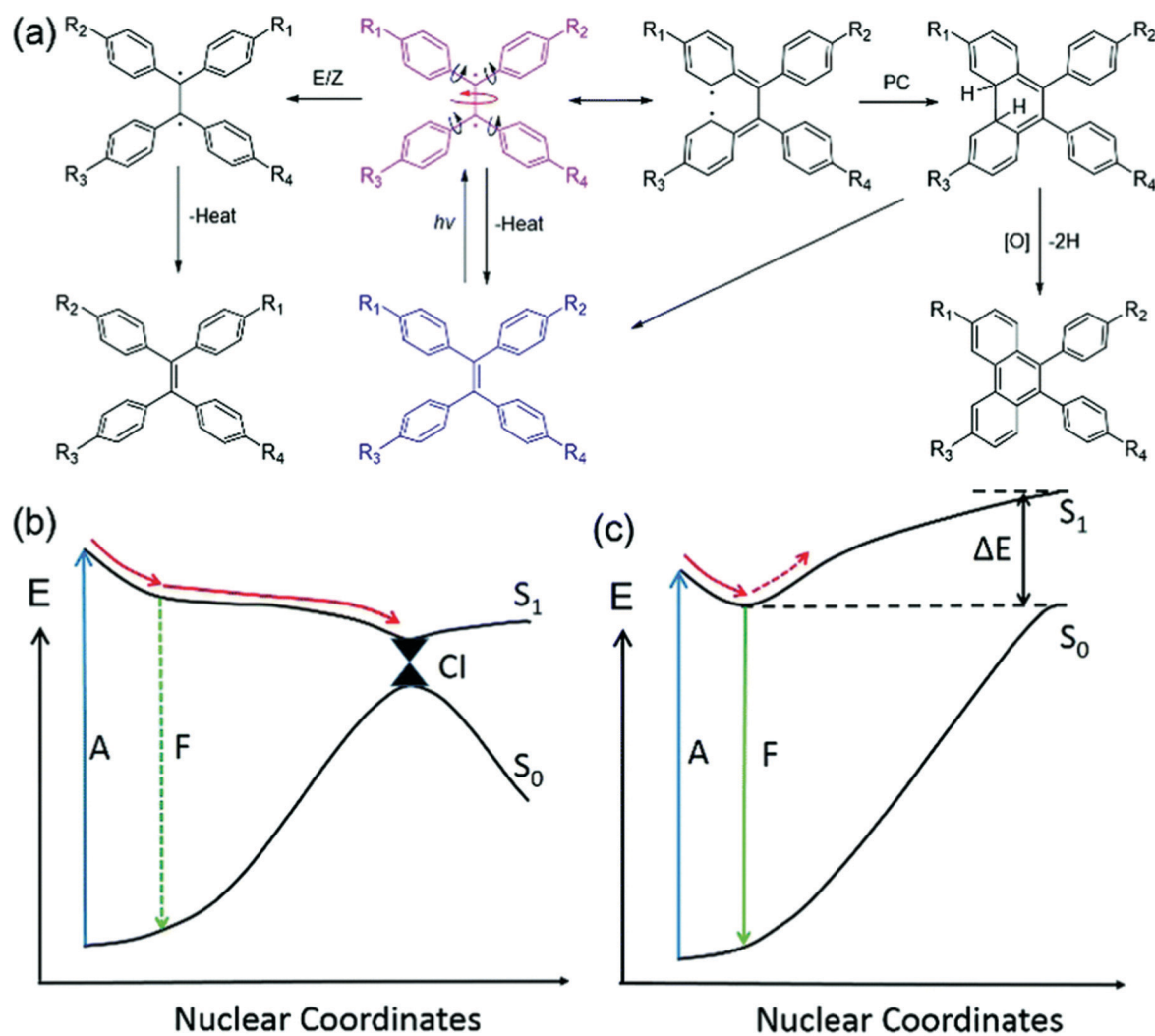


Fig. 2 (a) Simplified schematic illustration of the possible photophysical and photochemical processes of TPE derivatives. Proposed decay pathways along the potential energy curves of a typical AIE molecule in (b) solution with a low viscosity and (c) the solid or crystal state. Abbreviations: A = absorption, CI = conical intersection, and F = fluorescence. Reproduced with permission from ref. 8. Copyright 2019, Royal Society of Chemistry.

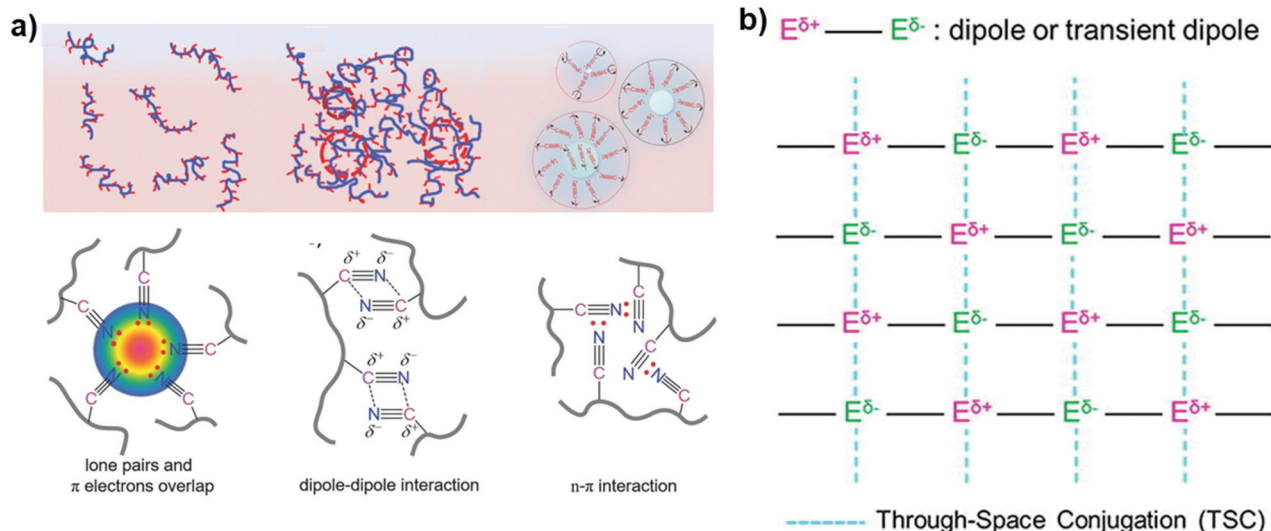


Fig. 3 (a) Schematic illustration of clusterization-triggered emission (CTE) and possible intra- and intermolecular interactions of PAN molecules. (b) Through-space conjugation (TSC) mechanistic image for clusteroluminescence. Figures reproduced with permission from (a) ref. 16. Copyright 2016, Wiley-VCH and (b) ref. 22. Copyright 2020, Elsevier Ltd.

However, these molecules do not possess extended π -electrons. For example, in 2007, Tang *et al.* reported that the non-aromatic poly[(maleic anhydride)-*alt*-(vinyl acetate)] showed blue fluorescence in its colloidal suspension but no fluorescence in dilute solution.¹⁴ A similar phenomenon and even efficient room-temperature phosphorescence were observed in natural compounds and polymers such as starch, cellulose, bovine serum albumin (BSA), and some other carbohydrates.¹⁵ In 2016, in work explaining the aggregation-induced emission (AIE) characteristics of non-conjugated polyacrylonitrile (PAN) molecules, clusterization-triggered emission (CTE) was first used to describe this phenomenon (Fig. 3a).¹⁶ Then, the theory of through-space conjugation (TSC; Fig. 3b) was proposed, by Tang, Yuan and co-workers, *i.e.* the clusterization of non-conventional chromophores with through-space conjugation results in extended electron delocalization and a rigid conformation – this has gradually come to be considered as the mechanism of this luminescence phenomenon.^{15,17–22} All the molecules form a whole *via* the through-space conjugation, while the whole rigidifies the conformation of all the molecules. As the saying goes: one for all, all for one.

The fluorescence of non-conjugated compounds is not a new phenomenon. As early as 1605, the mechanoluminescence of sugar was documented in the book *Advancement of Learning* by Sir Francis Bacon.²³ However, the CTE mechanism is conceptually new, and explains a large number of non-traditional intrinsic luminescence (NTIL) systems for which people have not previously realized the connection or have even misunderstood.^{21,23–34} And under the guidance of this concept, people have developed numerous of new systems.^{15,16,18–21,35–60} These NTIL emitters are called clusteroluminogens, and include small molecules,^{15,20,41,42,53,57,58,61–63} linear and hyperbranched polymers,^{16,18,19,28,33,36–38,43,44,46,48,49,52,55,60,63–78} biomacromolecules,^{29,35,47} supramolecules⁷⁹ and organic-inorganic hybrids.^{23,45,80,81} They generally contain N, O, S, P,

Si and other heteroatoms, including non-traditional chromophores such as hydroxyl ($-\text{OH}$),^{15,58} ether ($-\text{O}-$),^{42,65} carboxylic acid ($-\text{COOH}$),^{36,41,43,45} ester ($-\text{COOR}$),^{44,67} anhydride ($-\text{COOCO}-$),^{49,66,67} amide ($-\text{NHCO}-$),^{19,20,33,38,57,68,69,73,75,76,82} amine ($-\text{NH}_2$),^{72,74} nitrile ($-\text{CN}$),^{16,61} pyridine ($-\text{C}_5\text{H}_5\text{N}$),⁵² thioamide ($-\text{NHCS}-$),^{53,70} sulfide ($-\text{S}-$),^{18,62} sulfonate ($-\text{SO}_3\text{H}$),^{21,52,63,83} sulfoxide ($-\text{SO}$), sulfone ($-\text{OSO}-$),¹⁸ phosphate ($-\text{PO}_3-$),^{63,77} siloxane ($-\text{SiO}$),^{28,78,84} and so on. Some typical CTE structures are shown in Fig. 4, which will be collectively referred to as clusteroluminogens in the following discussions. Compared with traditional intrinsic luminescence (TIL) systems, clusteroluminogens usually have the advantages of good structural adjustability, convenient synthesis, high water solubility, and low biological toxicity. Many of them have been applied as green light-emitting materials and room-temperature phosphorescent materials, as well as in the field of biology.^{18,35,38,43,47,50–53,55}

In this review article, we aim to provide a systematic overview on CTE, including its mechanisms, processes, characteristics and applications. Finally, we envisage that the supramolecular self-assembly of the CTE system will become an important topic in the field of CTE study.

Mechanistic understanding of CTE

TSC model: through-space conjugation. According to Hohenberg–Kohn's first theorem, the electron density is the only factor that determines the properties of a molecule.^{85,86} Covalent bonds, ionic bonds and coordination bonds are just apparent forms of changes in the charge density caused by the interaction of atoms in a molecule. When there are non-bonded interactions in a system, although the effect of a single action is relatively weak, stacking them all, the charge density of the entire system will change, which in turn changes the optical, electrical, and magnetic properties of the system. In general, the greater the degree of delocalization of the system and the closer the two components are located, the stronger the interaction

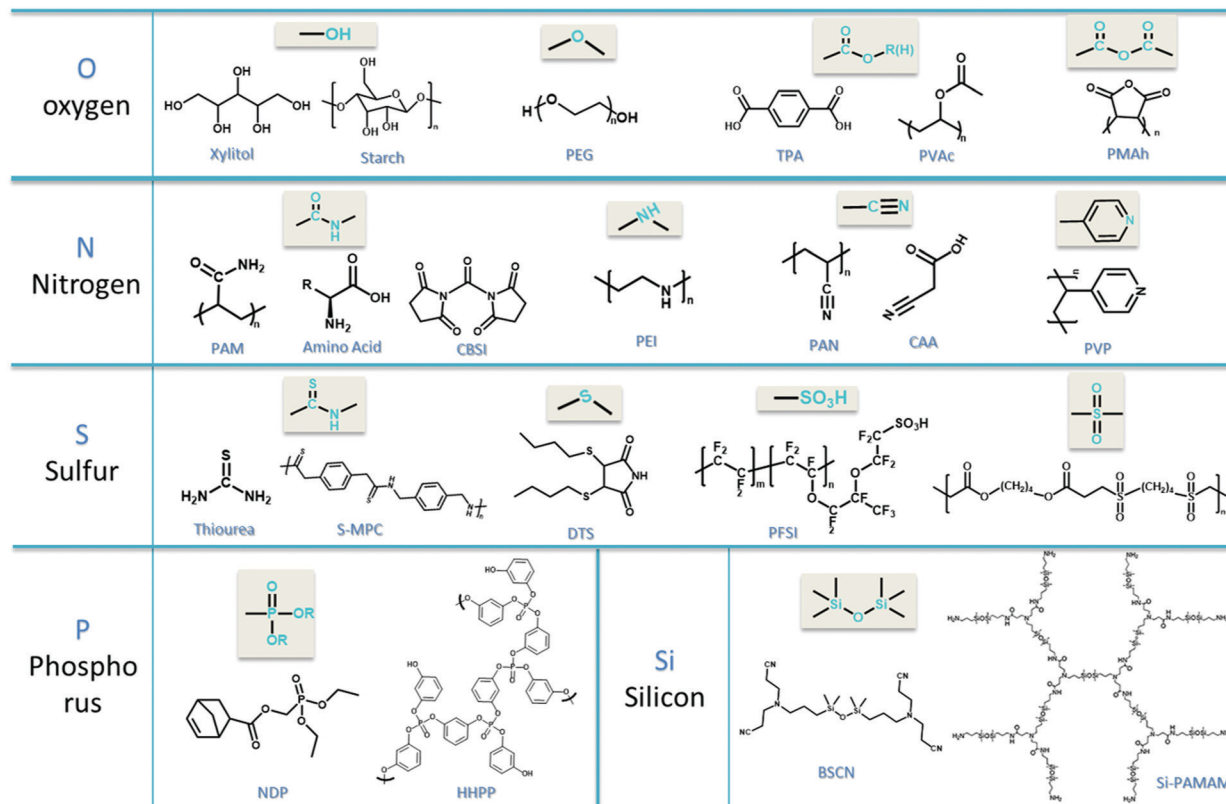


Fig. 4 Typical examples of CTE structures.

between them. In particular, for systems with electron-rich atoms, as long as the distance between the two atoms is appropriate, non-bonding interactions are likely to occur.

Therefore, we can easily understand the TSC model proposed and developed by Tang *et al.*²² and Yuan *et al.*^{17,21} In the CTE system, with the formation of clusters, a strong non-bonding interaction between the clusteroluminogens occurs, resulting in through-space conjugation (TSC) inside the cluster. As a result, the system exhibits fluorescence that is inaccessible by the isolated molecules. Fig. 5 schematically illustrates the TSC mechanism of CTE. For isolated heteroatom systems, the clusteroluminogen itself requires a great amount of energy (E_0) for the transition from the ground state (S_0) to the excited state (S_n/T_n). Furthermore, its intramolecular motions (rotation and vibration) are rapid. This means that non-radiative decay is very fast. Therefore, it is difficult to excite such a molecule, and luminescence can hardly be generated. By contrast, as the clusters are formed, clusteroluminogens with an atomic distance smaller than the van der Waals radius interact strongly. This leads to TSC and generates a narrow band gap (E_1) that allows the system to transit to an excited state (S'_n/T'_n) by absorbing UV light energy. Meanwhile, the intramolecular motions are restricted by the conjugate structure, and the energy of the exciton (S'_n/T'_n) is stabilized by restricting the structural relaxation. As a result, fluorescence and even phosphorescence transitions occur.

As a confirmation of the mechanism, Tang *et al.* synthesized oligo(maleic anhydride) (OMAh) and poly[(maleic anhydride)-*alt*-(2,4,4-trimethyl-1-pentene)] (PMP)⁸⁶ (Fig. 6). Experimentally, PMP displayed almost no fluorescence in either solution or the solid state. By contrast, the OMAh series exhibited blue and yellow emission in the solution and solid states, respectively, even for oligomers as small as $M_w \approx 1000$. Theoretical calculations reveal that the distance between two adjacent maleic anhydride (MAH) units in OMAh ranges between 2.84 Å and 3.18 Å, which forms a sub-van der Waals contact ($d < 3.22$ Å), rigidifies the oligomeric chain and increases the inter-/intra-chain interactions. Meanwhile, in PMP, the 2,4,4-trimethyl-1-pentene branches separate the neighboring succinic anhydride groups, and the optimized conformation of PMP shows a longer OC...OC distance of > 5 Å, thus preventing PMP molecules from undergoing TSC. The lack of TSC accounts for the lack of luminescence from PMP in both solution and clustered states.

More direct evidence was provided by a study on the solid-state molecular motion (SSMM) of two non-conjugated molecules: 1,2-diphenylethane (*s*-DPE) and 1,2-bis(2,4,5-trimethylphenyl)ethane (*s*-DPE-TM).⁸⁷ In the solid state, *s*-DPE shows intermolecular motion upon UV irradiation to form excited-state through-space complexes (ESTSCs) [Fig. 7(a)]. Radiative decay of the ESTSCs emits clusteroluminescence. Femtosecond transient absorption (fs-TA) spectroscopy provided direct evidence for the formation of ESTSCs, as illustrated by the occurrence of a new peak at 590 nm [Fig. 7(b)].

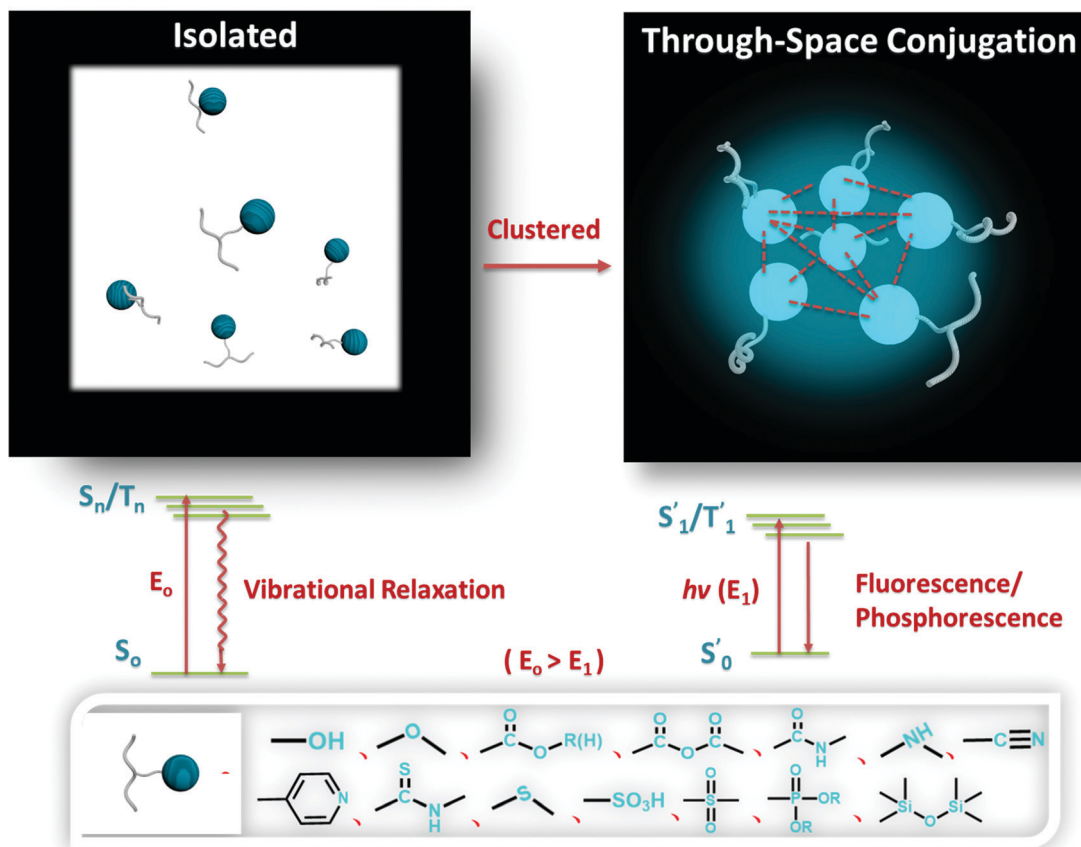


Fig. 5 Schematic illustration of the CTE mechanism.

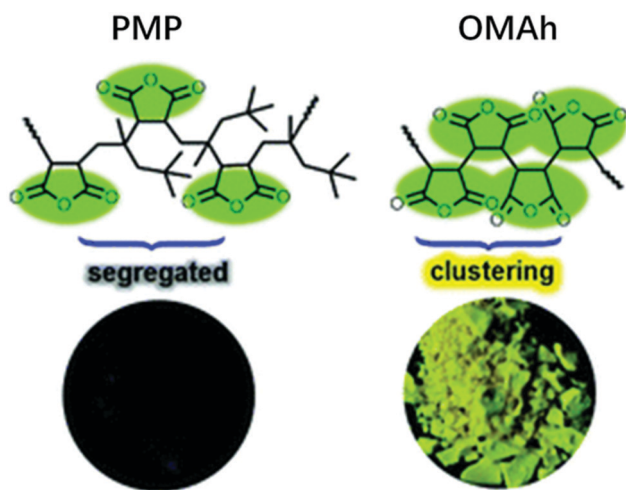


Fig. 6 Chemical structures of PMP and OMAh and images of PMP and OMAh in the solid state taken under 365 nm UV light irradiation. Reproduced with permission from ref. 86. Copyright 2017, Royal Society of Chemistry.

Structural characterization of CTE: single-crystal analysis and quantitative calculation

Generally speaking, the physical picture of TSC is the overlap of molecular orbitals, which is embodied by the fact that the distance between the non-conventional chromophores is

smaller than the van der Waals radius between them. Therefore, quantitative calculation and the single-crystal structure can be used as effective analytical tools to explain whether TSC exists or not.

For example, the CTE phenomenon of urea was studied by Yuan *et al.*⁵¹ As can be seen from Fig. 8(a and b), the urea molecule adopts a nearly planar conformation in the crystal. Notably, besides the typical (N-H...O=C) and atypical (N-H...C=O) hydrogen bonds, abundant H-N...O=C (2.971 and 3.044 Å) intermolecular short contacts are present, leading to well extended through-space conjugation. These intra/intermolecular electronic communications among electron-rich units constitute a 3D through-space electronic communication channel, which narrows the energy gaps and renders the clustered chromophores excitable by UV irradiation. Aiming to evaluate the electronic interactions of neighboring molecules, the HOMO and LUMO electron densities of the monomer, dimer, trimer, and tetramer of urea were calculated using the time-dependent density functional theory (TD-DFT). Despite the discrete electron distributions in the HOMO levels, evident electronic delocalization is present in their LUMOs [Fig. 8(c)], reflecting the enhanced conjugation in the clusteroluminogens.

N,N'-Carbonylbisuccinimide (CBSI) and *N,N'*-oxalylbis-succinimide (OBSI) also display typical CTE features. They are virtually non-luminescent in dilute solutions, while they are

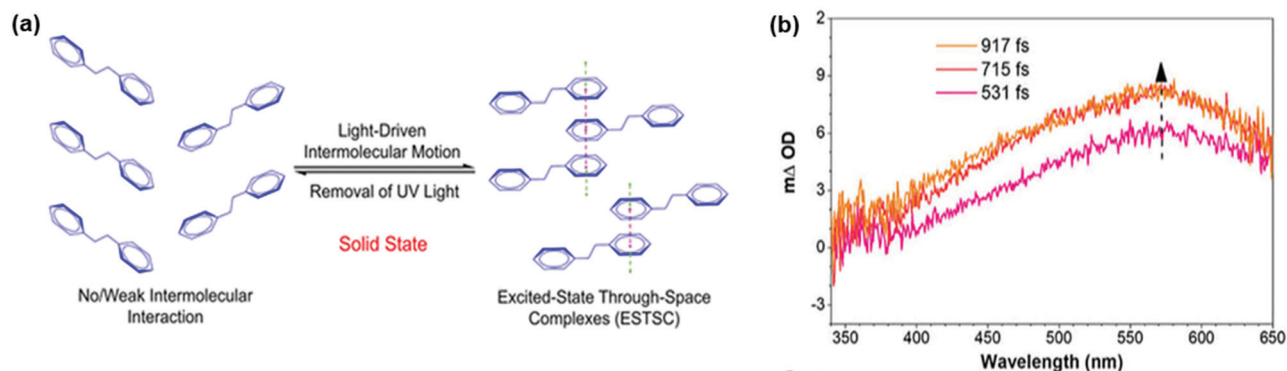


Fig. 7 (a) Schematic illustration of the light-driven intermolecular motion of *s*-DPE in the solid state. (b) fs-TA spectra of *s*-DPE in the film state with 267 nm excitation. Reproduced with permission from ref. 87. Copyright 2019, American Chemical Society.

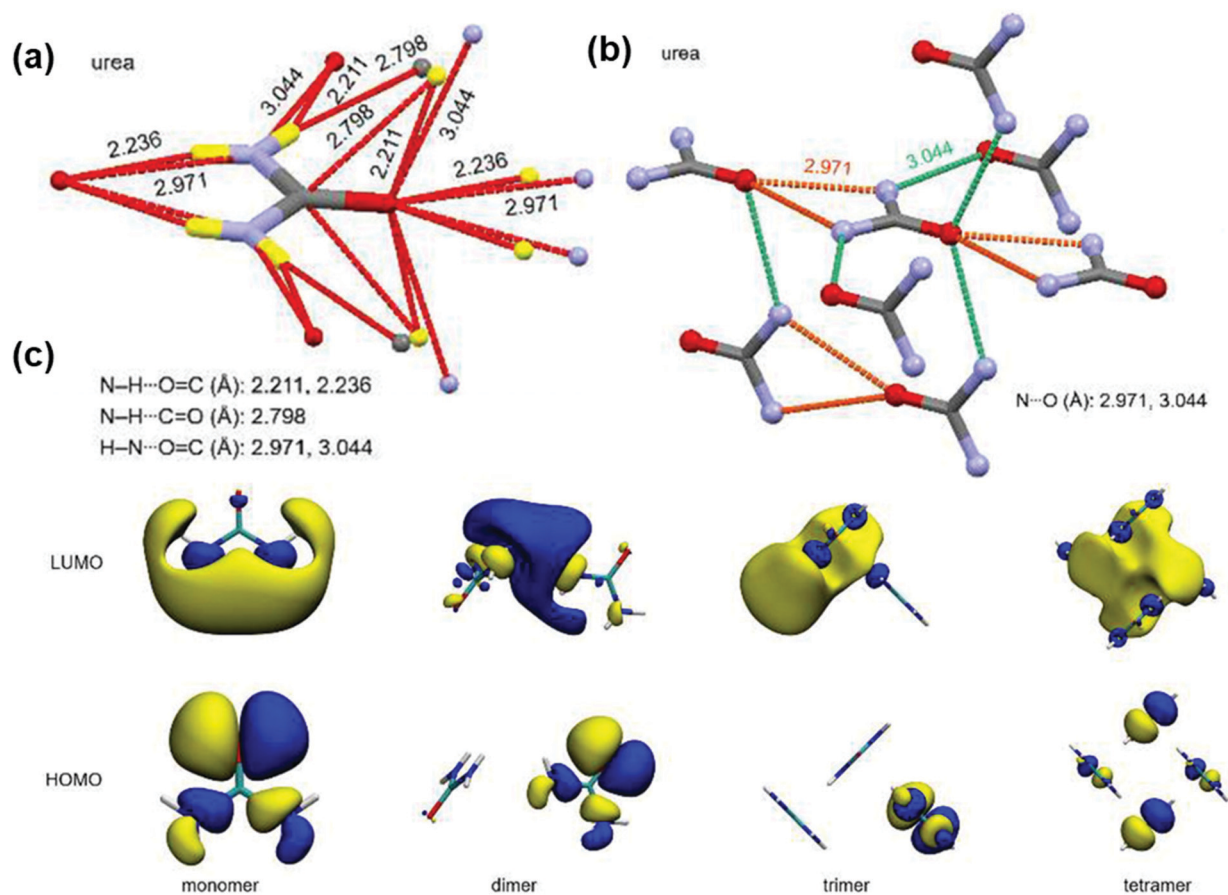


Fig. 8 (a) Single-crystal structure and (b) illustrated electronic communications between the N and O atoms around one molecule for urea. (c) Electron density distributions of the HOMO and LUMO levels of the monomer, dimer, trimer, and tetramer of urea. Reproduced with permission from ref. 51. Copyright 2019, Wiley-VCH.

brightly emissive in concentrated solutions or as crystals with a quantum yield (ϕ) of 9.0%.⁵⁷ The single-crystal structures of both compounds were determined at 298 or 173 K. As illustrated in Fig. 9(a and b), both compounds adopt highly distorted conformations in the crystal state. Short intermolecular distances such as C-H...O=C (2.453, 2.528, 2.639, 2.690, 2.702, and 2.714 Å), O=C...O=C (2.880, 3.035 and 3.159 Å), C-N...O=C (2.949 Å), and O=C...C=O (3.193 Å) are present. These short contacts, on

the one hand, remarkably stiffen the molecular conformations, but, on the other hand, facilitate 3D TSC among different moieties with n - and/or π -electrons. As depicted in Fig. 9(c), the HOMOs of an excited single molecule, a dimer, trimer and tetramer are all separated on the succinimide rings. However, intensive TSC amongst carbonyls and imides is noticed on their LUMOs.

It can be seen from the above examples that for small molecules, their crystal structures can be obtained, enabling

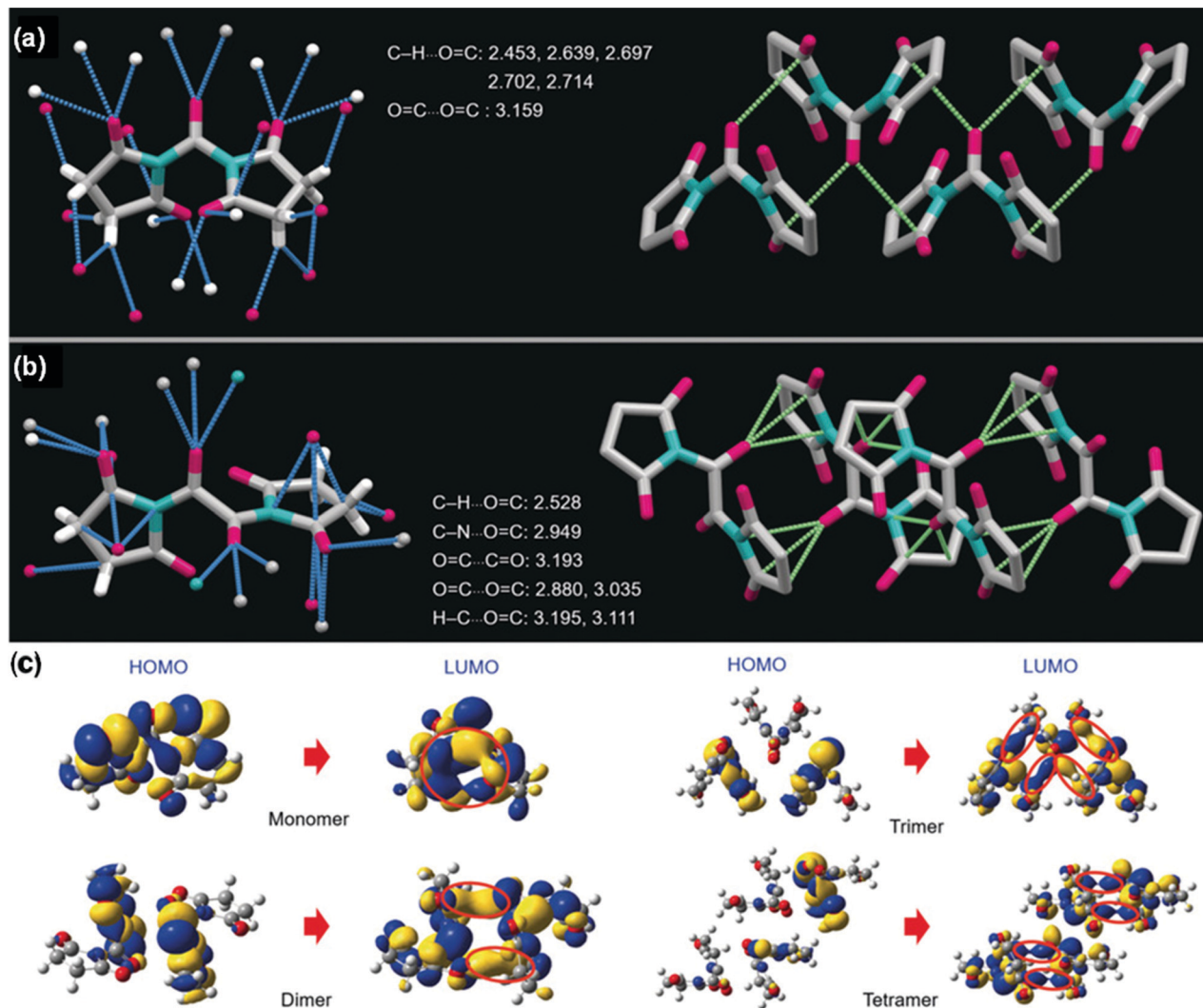


Fig. 9 Crystal structure (298 K) with denoted intermolecular interactions around one molecule and fragmental molecular packing with highlighted through-space conjugation for (a) CBSI and (b) OBSI. (c) Electron densities of HOMO and LUMO levels for the monomer, dimer, trimer, and tetramer of CBSI. Reproduced with permission from ref. 57. Copyright 2020, Wiley-VCH.

the determination of the relative position of each atom. This allows simulation of the orbital energy levels of their HOMOs and LUMOs for aggregates with different aggregation numbers, and the CTE effects can be confirmed. However, so far, more than half of the CTE systems have been found in polymers. For polymers, it is difficult to obtain their single-crystal structures and aggregation states. In this case, we can only look for the optimized molecular dynamics conformations. For example, in the study of the CTE effect of hyperbranched polysiloxane (HBPSi) and its cyclodextrin derivatives (HBPSi-CD), density functional theory (DFT) at the B3LYP/6-31G(d) level was used to optimize their conformations (Fig. 10).⁵⁰ The optimized conformation revealed that the HBPSi molecules formed aggregates driven by strong intermolecular H...O interactions (2.084, 2.851, 2.781, 2.726, 2.856, and 2.488 Å) and the N → Si and O → Si coordination bonds. Aggregate formation allows the electron-rich oxygen and nitrogen atoms to experience inter- and intramolecular O...O and O...N interactions. This facilitates the

overlap of lone pair (n) electrons in the aggregates, thus leading to electron delocalization and a decrease of the energy gap [Fig. 10(a)]. In comparison with HBPSi, HBPSi-CD has much stronger intermolecular hydrogen bonds, leading to larger through-space conjugation [Fig. 10(b)].

General characteristics of CTE

Concentration-enhanced luminescence. Concentration-enhanced luminescence refers to the phenomenon in which the luminescence of a chromophore solution is intensified with an increase in the concentration, which is opposite to the concentration-quenching effect of traditional dyes. Most CTE and AIE systems show significant concentration-enhanced luminescence effects due to the gradual formation of clusters or aggregates with increasing concentration. However, there is a fundamental difference in the mechanism between these two phenomena. For AIE molecules, the working mechanism is the restriction of intramolecular motions (RIM). Thus, besides aggregation or solidification, structural rigidification

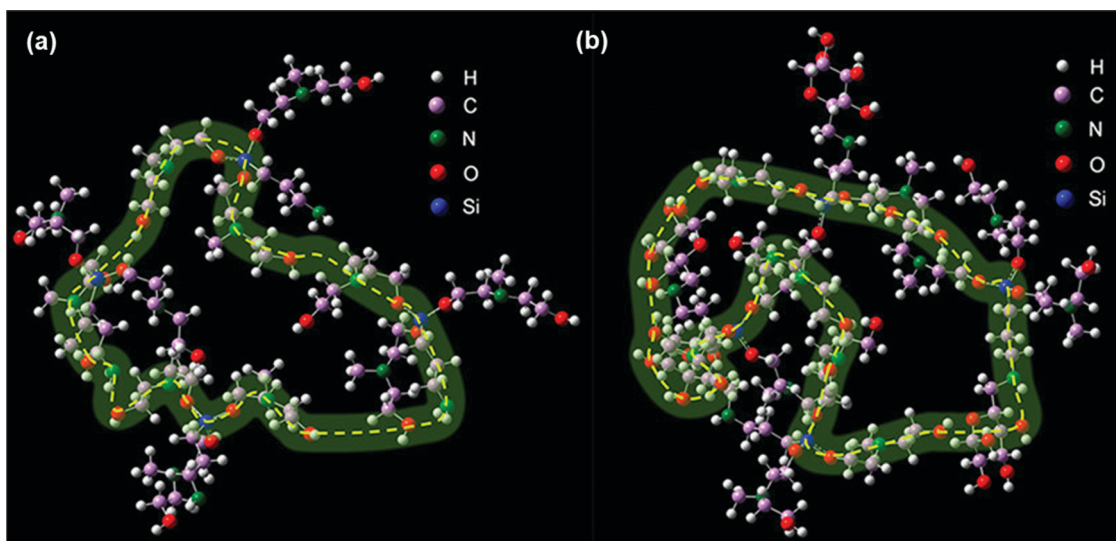


Fig. 10 Schematic diagrams of the through-space conjugation of HBPSi (a) and HBPSi-CD (b) (first generation, four molecules). Reproduced with permission from ref. 50. Copyright 2019, American Chemical Society.

in highly viscous media, at low temperature, by adsorption onto a solid surface or through doping into a rigid matrix can also lead to strong emission. Aggregation is not necessary for strong emission.⁸ By contrast, clusterization is firmly a prerequisite for through-space conjugation.

The typical CTE effect can be directly observed by comparing the fluorescence intensity values of a CTE system at different concentrations. For instance, the dilute DMF solutions ($\leq 1 \text{ mg mL}^{-1}$) of the non-aromatic polyurethanes (PUs) bearing carbamate (NHCOO) groups are non-luminescent under 365 nm UV irradiation (Fig. 11), which is ascribed to isolation of the

NHCOO groups along the polymer chains.¹⁹ However, weak but visible emission is detected as the concentration is increased to 5 mg mL^{-1} , and much brighter luminescence with remarkable enhancement is noticed at 50 mg mL^{-1} . Spectral measurements reveal that the emission maximum is 433 nm with a shoulder at 491 nm [excitation wavelength (λ_{ex}) = 365 nm]. These emissions should originate from the NHCOO clusters with rigidified conformations.

How can the relationship between the concentration and clusters in a CTE system be studied experimentally? For polymers, variation of the solution viscosity is very informative since the

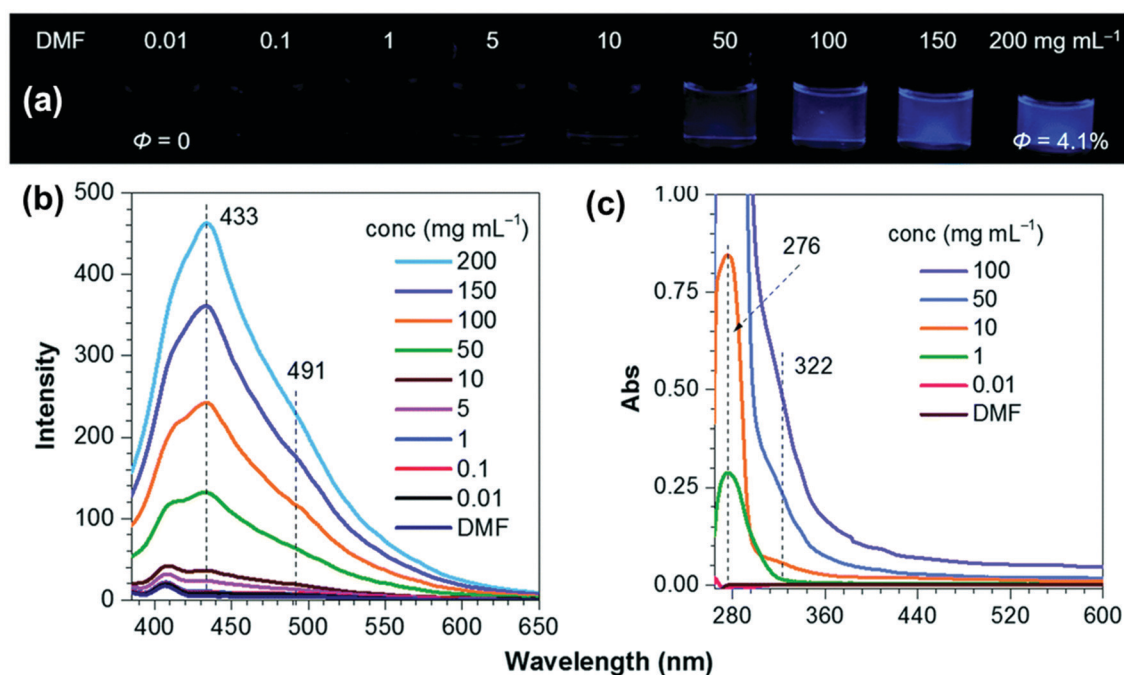


Fig. 11 (a) Images taken under 365 nm UV light, and (b) emission and (c) absorption spectra of different PU₄/DMF solutions. Reproduced with permission from ref. 19. Copyright 2018, Royal Society of Chemistry.

solution viscosity is related to the physical network formed by the polymers. In a study on the CTE effect of sodium alginate (SA) by Yuan *et al.* in 2018,⁴³ the shear viscosity as well as the storage (G') and loss (G'') moduli of SA solutions were found to correlate well with the photophysical processes of CTE. They first the relationship between the specific viscosity (η_{sp}) and the concentration (C) was plotted to establish the different concentration regimes (Fig. 12). The parameters C^* , C_e and C_D denote the intersections between the neighboring concentration regimes, namely, the successive dilute, semidilute unentangled, semidilute entangled, and concentrated regions. C_e characterizes the onset of significant overlap between the polymer chains where the macromolecular chain motion is topologically constrained. As for C_D , it marks the onset of the concentrated regime. The scaling relationships between the viscosity and concentration of SA ($M_w = 320\,000$, PDI = 2.1, and $M/G = 1.53$) are obtained as $\eta_{sp} \approx C$, $\eta_{sp} \approx C^{1/2}$, $\eta_{sp} \approx C^{3/2}$, and $\eta_{sp} \approx C^{33/10}$ for the dilute, semidilute unentangled, semidilute entangled, and concentrated regions, respectively. In the dilute solutions ($C < C^*$), except for possible intramolecular O...O contacts in the G (C-5 epimer α -L-guluronic acid) and M (1,4-linked β -D-mannuronic acid) moieties, rigid and extended worm-like chain conformations result in the isolation of oxygen atoms and carboxylate groups without sufficient electronic conjugation. As the concentration reaches the semidilute entangled region ($C_e < C < C_D$), the SA chains can “enter” the domain occupied by other molecules, thus facilitating the contact of

neighboring oxygen atoms and carboxylate units. This entangled region also coincides with the appearance of faint emission from the 0.5 wt% solution, indicating the crucial role of clusterization of non-conventional chromogenic groups in the emission. The emission becomes much stronger as the aqueous solutions approach the concentrated regime $C > C_D$. At this stage, the scaling relationship of SA approximates those of the neutral polymers since the electrostatic charges are screened with the overlap of electrostatic droplets. Aided by the close packing of SA chains, oxygen atoms and carboxylate moieties are clustered in close proximity, resulting in the efficient overlap of n and π electrons along with extended electronic conjugation and simultaneously rigidified conformations, thereby endowing these clusteroluminogens with boosted emissions.

Excitation wavelength dependence

Most CTE displays excitation-wavelength-dependent emission. Because the size and structure of the clusters formed in a CTE system are often diverse, each clusteroluminogen has a different spatial environment, and the interaction between them is also different. This means that nearly every clusteroluminogen is an independent emission species in the system with different excitation and emission wavelengths. For instance, in the study of D-Xylose (D-Xyl), a saccharide with multiple hydroxyl groups,⁵⁸ the clusterization of lone pairs (n) and/or π electrons yields clusteroluminogens with varied extended electron delocalization.

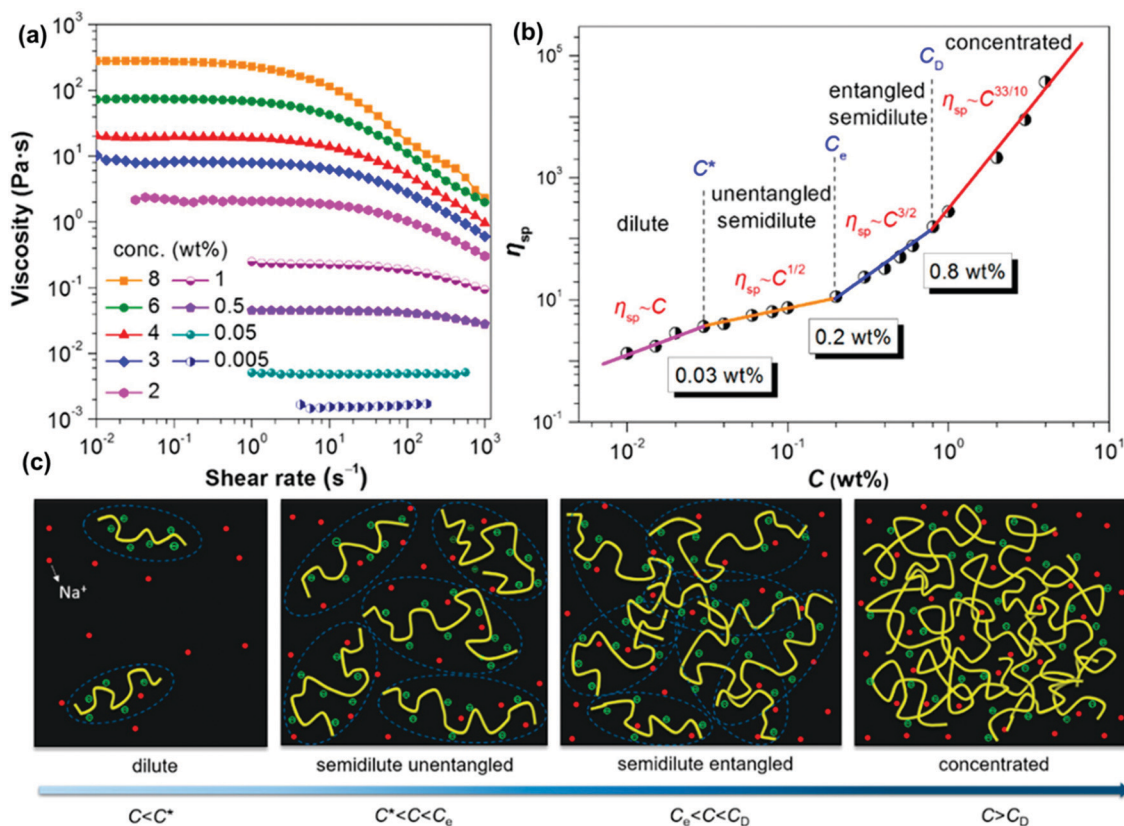


Fig. 12 (a) Viscosity of varying SA aqueous solutions at different shear rates. (b) The plot of η_{sp} versus the concentration of SA solutions. (c) Schematic illustration of the chain conformations of SA in varying solutions. Reproduced with permission from ref. 43. Copyright 2018, American Chemical Society.

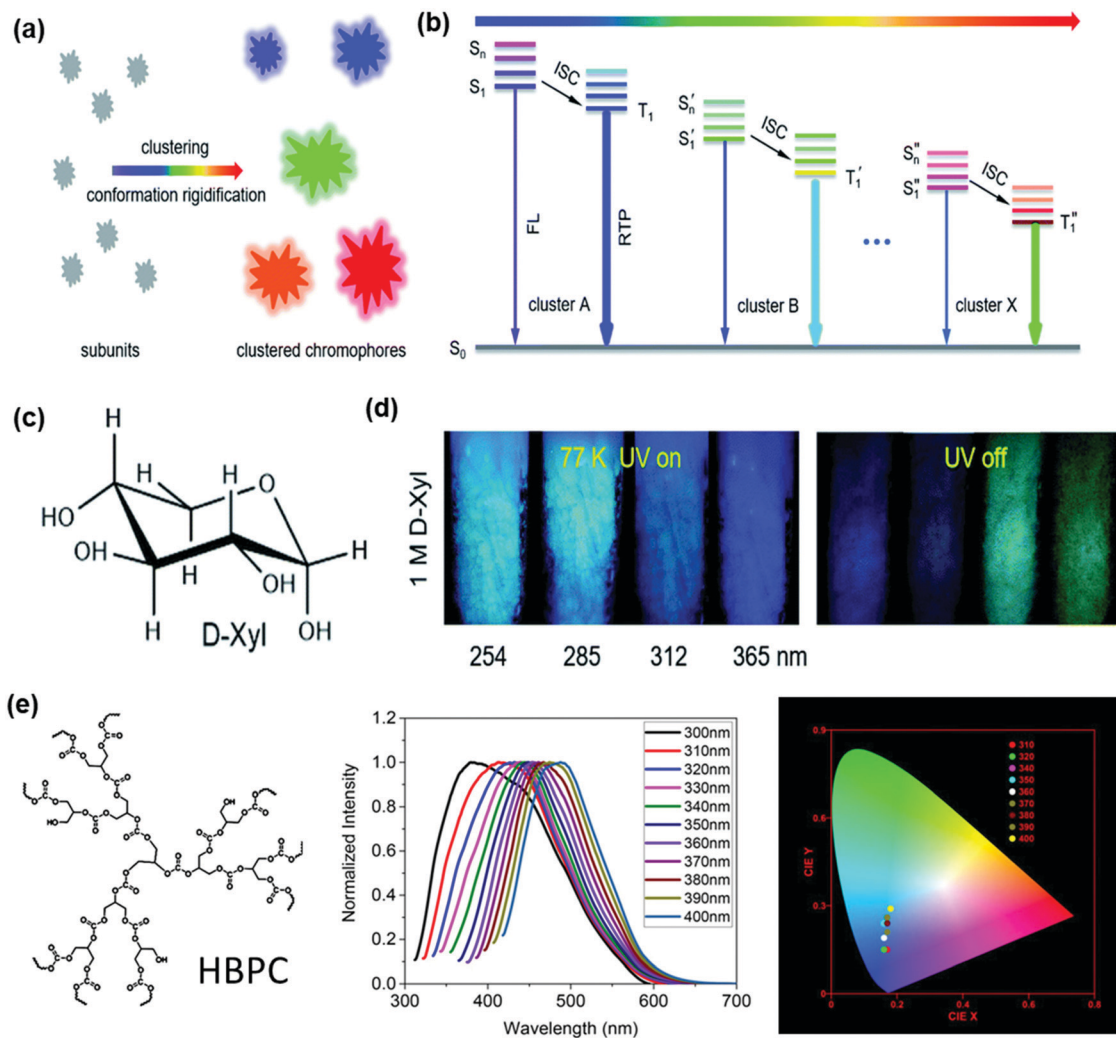


Fig. 13 (a) Schematic illustration of the CTE mechanism of non-conventional luminogens. (b) Jablonski diagram for the demonstration of colour-tunable luminescence in non-conventional luminogens. (c) Structure of *D*-Xyl. (d) Images of a 1 M *D*-Xyl solution taken at 77 K under the illumination of various UV light wavelengths or upon stopping the UV irradiation. (e) Structure of HBPC, and normalized fluorescence spectra and CIE chromaticity coordinates for HBPC at a concentration of 12 mg mL⁻¹ in aqueous solution at a series of excitation wavelengths with a 10 nm increment. Figures reproduced with permission from (a)–(d) ref. 58. Copyright 2020, Royal Society of Chemistry, and (e) ref. 44. Copyright 2017, Wiley-VCH.

This generates λ_{ex} -dependent emission [Fig. 13(a and b)]. Upon freezing to 77 K, the emission color of the concentrated *D*-Xyl solution (1 M) changed from cyan to blue as the λ_{ex} value was varied from 254 to 365 nm [Fig. 13(d)]. Detailed spectral analysis suggested that this emission color change originates from ratio-metric variation among the emission maxima/shoulders at 393, 443 and 462 nm. Similar excitation-wavelength-dependent CTE colors were also found in other systems. A typical example is the CTE of HBPC.⁴⁴ As the excitation wavelength of HBPC is increased, the emission wavelength exhibits a progressive red shift [Fig. 13(e)].

Room-temperature phosphorescence (RTP)

Pure organic room-temperature phosphorescence (RTP) has been actively demonstrated to have immense potential for specific applications, including organic optoelectronics,^{88–92} anti-counterfeiting labelling for advanced data security,^{93–95} highly sensitive sensing,^{96–98} and high-contrast time-gated *in vitro* and *in vivo*

imaging.^{99–103} However, RTP from pure organic emitters remains challenging since the intersystem crossing (ISC) process and the phosphorescence lifetime depend highly on the efficiency of spin–orbit coupling (SOC), as well as on the prominent effect of oxygen quenching on the triplet excited state.¹⁰⁴

However, in CTE systems, the RTP phenomenon is often observed.^{16,18–20,35,37,38,42,43,51} This is because there are abundant heteroatoms in CTE systems, and the heteroatoms are known to enhance SOC, thereby promoting ISC. Furthermore, TSC in the CTE system provides a rigid environment that greatly increases the excited-state lifetime. Finally, the TSC effect can be further improved by ionization of the CTE molecules since ions may enhance the polarization of the CTE system, which is called the polarization-enhanced conjugation effect.

For example, the amorphous non-aromatic polymers of poly-(acrylic acid) (PAA), polyacrylamide (PAM) and poly(*N*-isopropyl-acrylamide) (PNIPAM) were found to display persistent RTP.³⁸

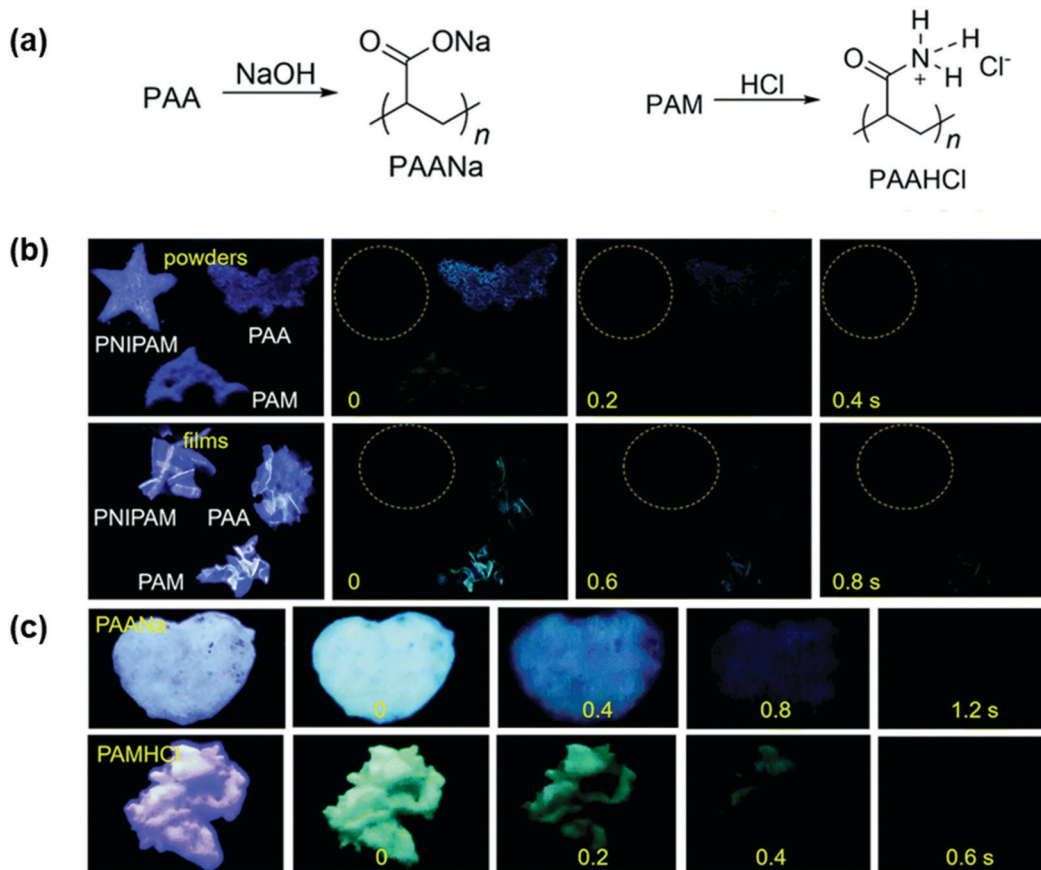


Fig. 14 (a) Structure of PAANa and PAMHCl. (b and c) Images of different powders and films taken under 312 nm UV light or after ceasing UV irradiation. Reproduced with permission from ref. 38. Copyright 2019, Royal Society of Chemistry.

PAA/PAM powders and films demonstrate cyan RTP after ceasing the UV irradiation [Fig. 14(b)], with emission maxima (λ_{em}) and lifetime ($\langle\tau\rangle_p$) values of 488/482, 504/489 nm and 41.8/97.6, 54.4/117.0 ms, respectively. Upon neutralization with NaOH or fuming with HCl, the resulting PAANa and PAMHCl powders show a greatly enhanced emission efficiency and a prolonged RTP lifetime [Fig. 14(c)], with $\Phi/\langle\tau\rangle_p$ values of 7.6%/139.1 ms and 16.7%/116.9 ms, respectively. In another study, persistent RTP was observed in the powders of ϵ -poly(L-lysine) (ϵ -PLL) after ceasing UV irradiation.¹⁹

Polarization-enhanced luminescence

Inter/intramolecular electrostatic interactions produced by a dipole or transient dipole serve as an important driving force for the formation of clusteroluminogens.²² As the polarization enhances the relative strength of the spatial conjugation and further stabilizes the conformation of the clusters, polarization can enhance the efficiency of CTE.

For example, poly(4-vinylpyridine) (PVP) is a typical CTE polymer with weak RTP. In the work reported by An *et al.*, upon ionization with different organic acids, PVP-based ionization products showed distinct phosphorescence behavior.⁵² Under ambient conditions, heavy-atom-free poly(4-vinylpyridine)butane-1-sulfonate (PVP-S) exhibits an emission lifetime of up to 578.36 ms,

which is 525 times longer than that of the original PVP. The strong ionic interactions between sulfonic acid and PVP played a critical role in boosting ultralong phosphorescence in PVP-S by suppressing the non-radiative transitions and restricting the chromophore motions [Fig. 15(a)]. The effects of different anions on PVP-based ionization products are also reported. Between the PVPs carrying chloride (PVP-C) and bromide (PVP-B) counterions, PVP-B exhibited a longer phosphorescence lifetime [Fig. 15(b)] since the bromine ions show greater polarizability and possibly a stronger heavy-atom effect than chloride ions.

Impressive examples of CTE systems

Biomacromolecules. One of the most important values of CTE theory is changing people's understanding of protein luminescence in organisms. It is textbook knowledge that protein photoluminescence stems from the three aromatic amino acid residues of tryptophan (Trp), tyrosine (Tyr), and phenylalanine (Phe), with predominant contributions from Trp.^{105–107} However, Yuan *et al.* have revisited the emission of natural proteins using BSA as the representative.³⁵ BSA consists of 583 amino acids in a single polypeptide chain with a molecular weight of around 66 kDa and has a heart-shaped structure at physiological pH [Fig. 16]. The photophysics of BSA revealed new aspects of protein photoluminescence: (1) other

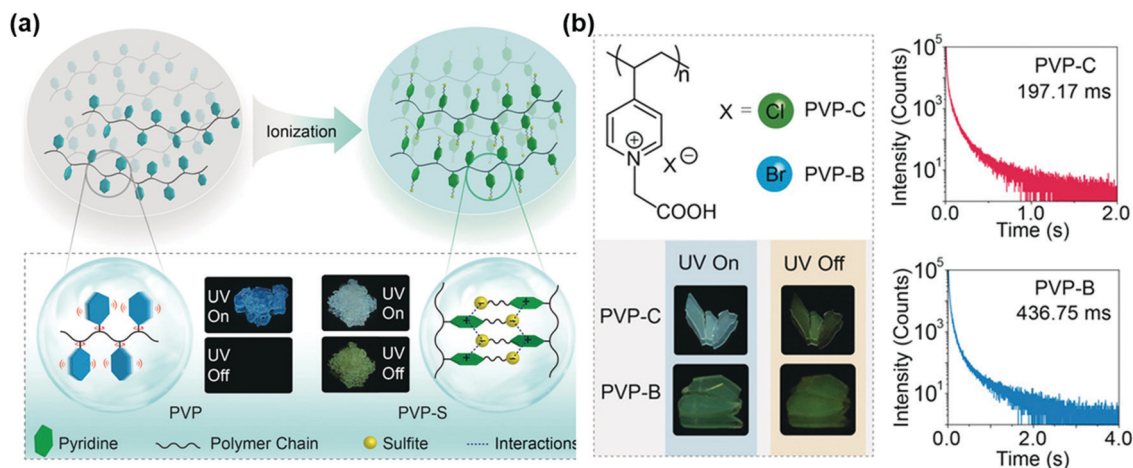


Fig. 15 (a) Ionization enabling ultralong organic phosphorescence in polymers. (b) Photophysical properties of ionized PVP-B and PVP-C polymers in the solid state. Reproduced with permission from ref. 52. Copyright 2019, Wiley-VCH.

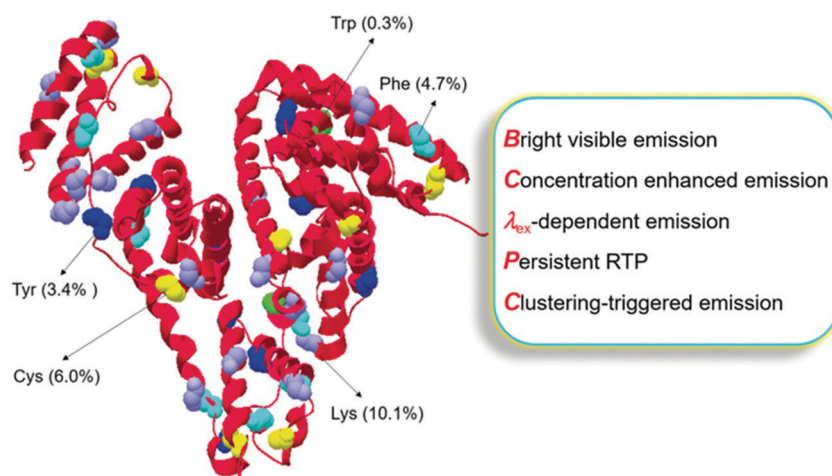


Fig. 16 BSA structure with partial aromatic (green, cyan, and blue) and non-aromatic (purple and yellow) amino acid residues shown in different colours. Reproduced with permission from ref. 35. Copyright 2019, Wiley-VCH.

than the UV emission from Trp residues, BSA can generate intense λ_{ex} -dependent visible PL upon concentration or aggregation; (2) RTP with a lifetime value ((τ_p)) of up to 34 ms is acquired in air from BSA in the solid state despite its amorphous nature; and (3) this unique visible emission and RTP are readily enhanced through further pressurization. All these results are highly related to the contribution of non-aromatic moieties, including the polypeptide backbone and diverse pendant groups, and are understandable in terms of the CTE mechanism.

Multicolour luminescent polymers

Although the emission wavelength of a typical CTE system changes with the excitation wavelength, its luminescence window is often in the blue region (400–480 nm). However, several systems have been published with an emission beyond blue, even showing red fluorescence.^{54,56,108–110} For example, the variation in fluorescence during the process of heat treatment of hyperbranched (HP)-PAMAM was studied.¹⁰⁸ Upon heating at 90 °C, the colourless pristine HP-PAMAM gradually turned

pale yellow and became luminescent. Fig. 17 displays the contour plots of excitation–emission matrices (EEMs) measured at different time points in the heating process. Gradual changes in the spectral shift and emission intensity were observed. Subsequently, bright yellow fluorescence was obtained after 18 h of heating.

In another study, orange–red and bright white emissions under 365 nm UV irradiation were observed in poly(itaconic anhydride-co-vinyl caprolactam) (PIVC) and poly(itaconic anhydride-co-vinyl pyrrolidone) (PIVP) copolymers⁵⁴ [Fig. 18]. The copolymers show concentration-dependent luminescence, and their emissions change from blue to orange with an increase in the polymer concentration. In addition, they also exhibit significant excitation-dependent fluorescence characteristics and emit dark red light when excited with red light.

Organic–inorganic hybrid materials

Organic–inorganic hybrid materials are emerging as attractive CTE materials. Many organic CTE groups may interact with inorganic nanoclusters through chemical bonding or physical

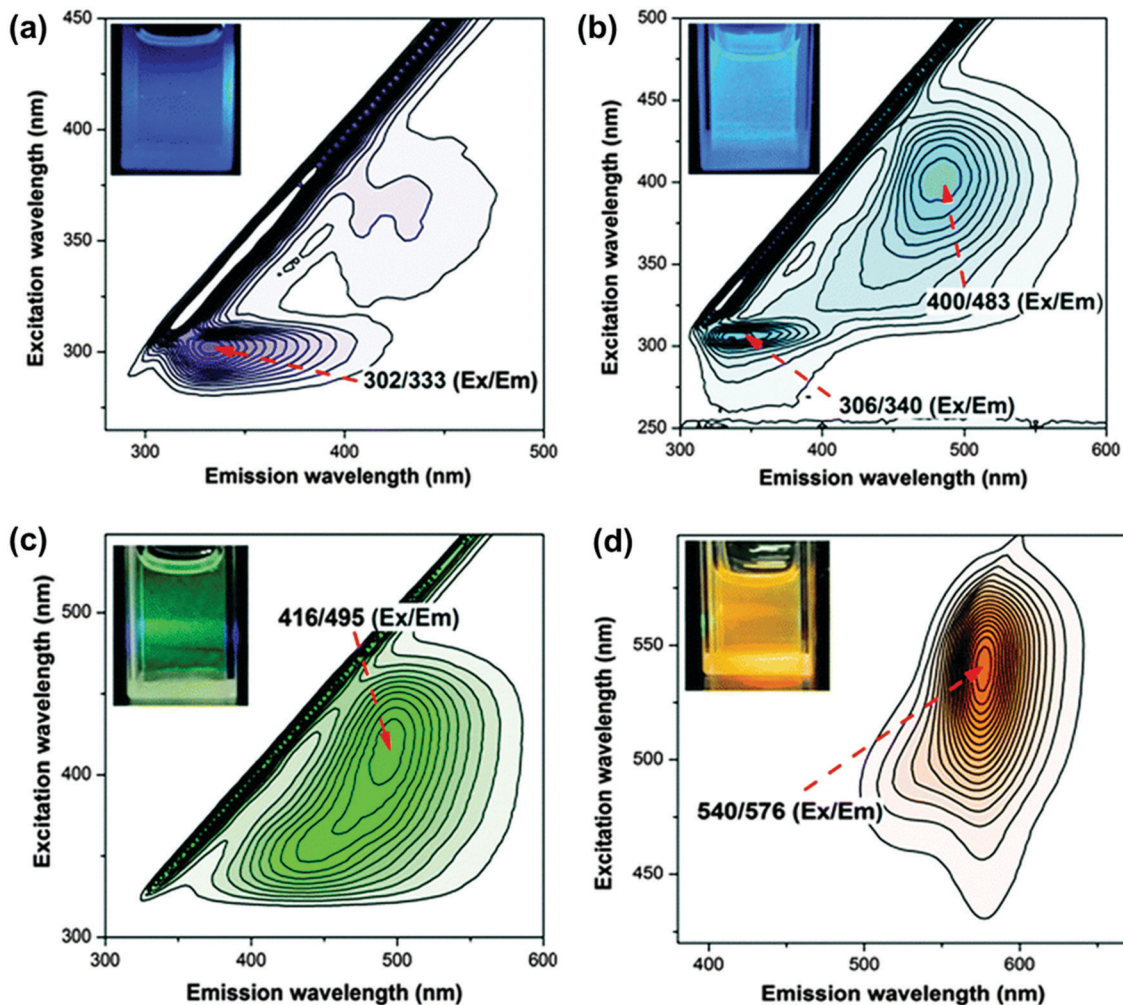


Fig. 17 Contour plot for the fluorescence EEMs of HP-PAMAM measured during the heating process: (a) 0, (b) 4, (c) 12 and (d) 18 h. Red arrows indicate the position of fluorescence peaks. Insets in (a)–(d) are images of the corresponding samples under irradiation of their respective maximum excitation wavelengths. Reproduced with permission from ref. 108. Copyright 2014, Royal Society of Chemistry.

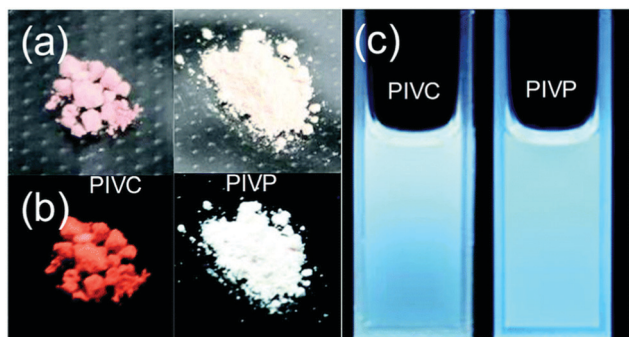


Fig. 18 Images of the solid powders of PIVC and PIVP under (a) natural light, (b) 365 nm UV light, and (c) their DMSO solutions ($C = 2 \times 10^{-4} \text{ g mL}^{-1}$) under 365 nm UV light. Reproduced with permission from ref. 54. Copyright 2020, Royal Society of Chemistry.

admixing. These hybrid materials present richer luminescence properties than pure organic systems.^{45,81,111–118} On the one hand, the inorganic clusters serve as the platform for the

clusterization of organic functional groups; on the other hand, they provide a large number of free electrons to participate in the TSC process, which greatly broadens the luminescence range and improves the emission efficiency. At the same time, metal clusters such as Au clusters and Ag clusters with excellent luminescence properties can have a synergistic effect with the fluorescence of CTE. For example, the luminescence of *D*-penicillamine (DPA)-capped silver nanoclusters (DPA-AgNCs) was studied [Fig. 19(a)].¹¹⁹ Metal-centered emission (MCE) and ligand-centered emission (LCE) were simultaneously observed in AgNCs. The contributions of the metal core and surface ligands were systematically investigated. The MCE was ligand-independent and has relatively lower photoluminescence quantum yields (QYs). By contrast, the LCE was highly ligand-dependent and exhibited a ligand synergistic effect with unique pH-dependent emission.

Furthermore, the organic–inorganic hybrid cluster itself can be used as a clusteroluminogen. When the cluster is further clustered, it forms a “cluster of clusters”, which produces a

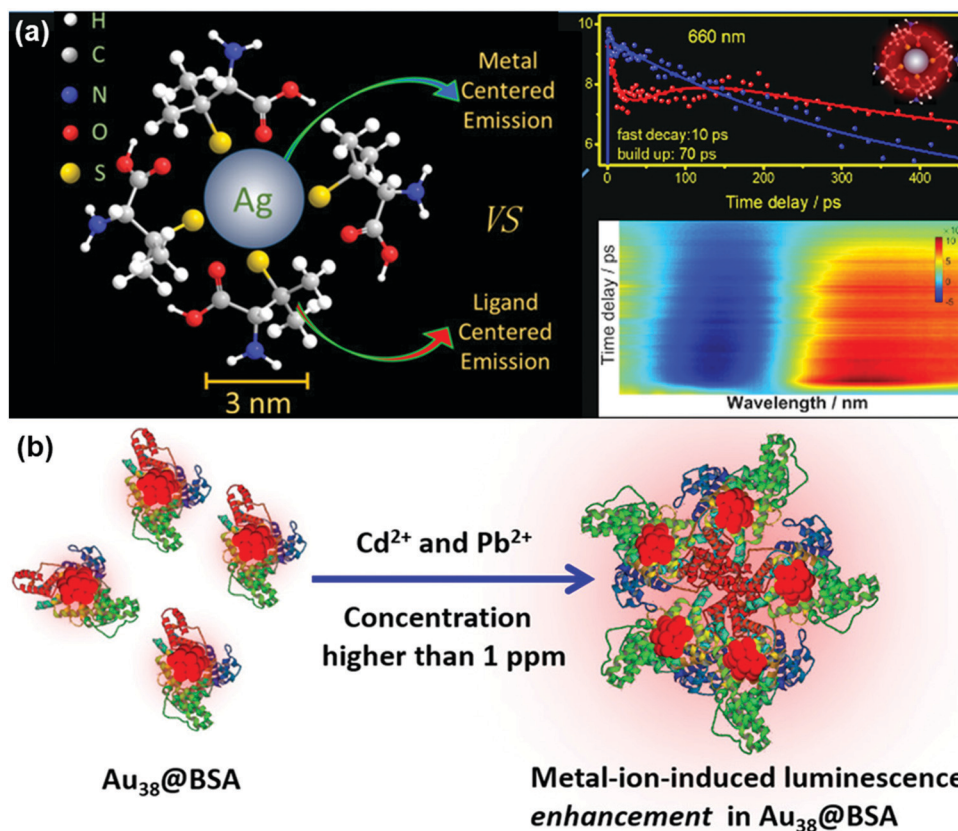


Fig. 19 (a) Schematic illustration of metal-centered emission versus the synergistic effect in ligand-centered emission. (b) Schematic illustration of aggregation-induced emission enhancement in protein-protected gold clusters of Au₃₈@BSA. Figures reproduced with permission from (a) ref. 119. Copyright 2019, American Chemical Society and (b) ref. 120. Copyright 2019, American Chemical Society.

supramolecular CTE effect. For example, the luminescence of Au₃₈@BSA and the aggregates of Au₃₈@BSA were studied [Fig. 19(b)].¹²⁰ When the Au₃₈@BSA cluster was excited at 365 nm, two emission maxima were found: one at around 450 nm, which is due to weak luminescence from the protein, and the other at 645 nm because of emission from the cluster. Then, in the presence of Cd²⁺ and Pb²⁺, for concentrations higher than 1 ppm, Au₃₈@BSA was found to have aggregation-induced emission enhancement. The luminescence enhancement was due to the aggregation of clusters, as detected by DLS and HRTEM analyses.

Applications of CTE materials

Through the previous introduction, we can roughly see the superiority of CTE materials. The multi-colour luminescence of CTE materials gives them special advantages in traditional fluorescent applications such as fluorescent coatings⁵⁷ and optoelectronic materials.⁵⁶ Moreover, CTE materials often exhibit excellent biocompatibility, thus showing advantages in the field of biological fluorescent labeling.^{19,38,43,50,55} Most importantly, the mechanism of CTE determines that materials are highly sensitive to external stimuli. Any stimulus that changes the aggregation state of the CTE material can obtain a corresponding response on fluorescence, rendering them excellent sensors.^{19,37,42–44,60} In this section, we will introduce some examples based on the above three points.

Anti-counterfeiting materials

One of the important applications of CTE materials is in anti-counterfeiting. Both the multicolour and RTP properties of CTE materials are beneficial in creating multilevel anti-counterfeiting patterns. For example, the powder form of *N,N'*-carbonylbis-succinimide (CBSI) displays CTE.⁵⁷ As shown in Fig. 20, the word “ON” was composed of conventional luminescent terephthalic acid (TPA) and CBSI solid powders, respectively. Under 312 and 365 nm UV irradiation, the “ON” of TPA powder shows a consistent deep-blue emission while its CBSI counterpart glows yellowish white and bluish white, respectively. Furthermore, the multicolour RTP feature of CBSI makes the corresponding pattern exhibit distinct green and yellow afterglows after ceasing the 312 and 365 nm UV irradiation, whereas the former pattern of TPA shows an unchanged greenish yellow colour. This colour-tunable emission characteristic makes CBSI a promising multilevel security material. Obviously, the λ_{ex} -dependent PL and RTP of CTE materials are more advantageous in anti-counterfeiting than traditional afterglow materials.

White LED materials

Phosphor-converted white LEDs have shown their superiorities in the consumption of electricity, lifespan, and colour rendering index (CRI),¹²¹ especially for the single white-light-emitting

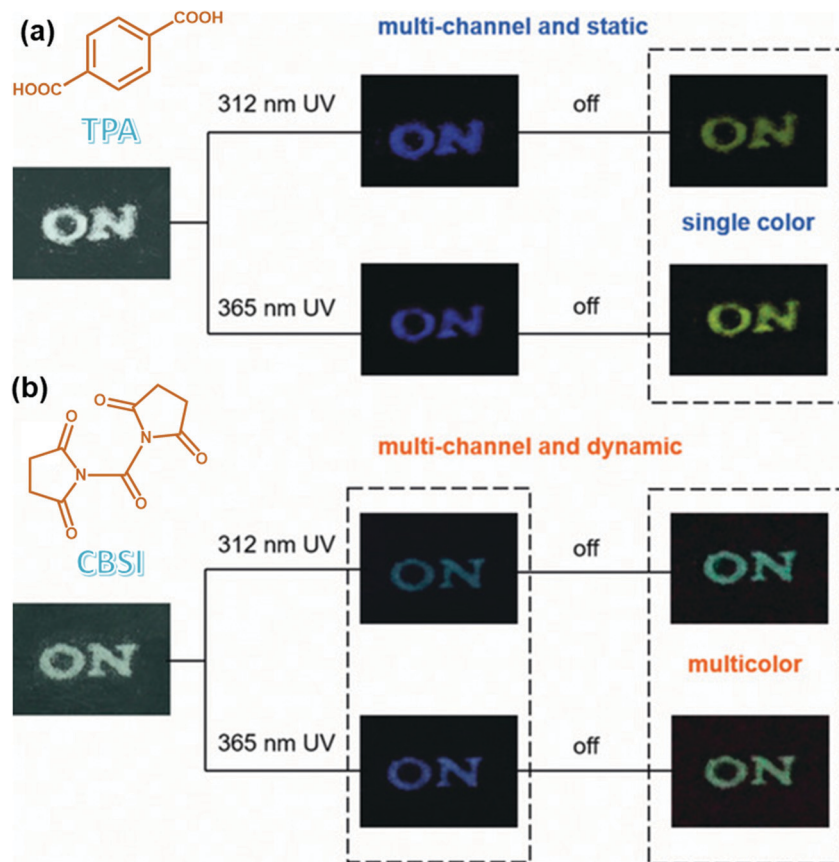


Fig. 20 Anti-counterfeiting applications with the word “ON” using (a) TPA and (b) CBSI solid powders. Reproduced with permission from ref. 57. Copyright 2020, Wiley-VCH.

phosphor. In the work published by Zhang *et al.*,⁵⁶ white LEDs with a high CRI of 95 were fabricated by combining PHUMs-180 [poly(hydroxyurethane) microspheres prepared at 180 °C] as a single phosphor with a UV chip. The white-light-emitting PHUMs

containing CTE materials were prepared *via* crosslinking of trimethylolpropane tri(cyclic carbonate) ether and 1,6-hexanediamine in chloroform [Fig. 21(a)], and the emission colour of the PHUMs could be controlled by changing only the reaction

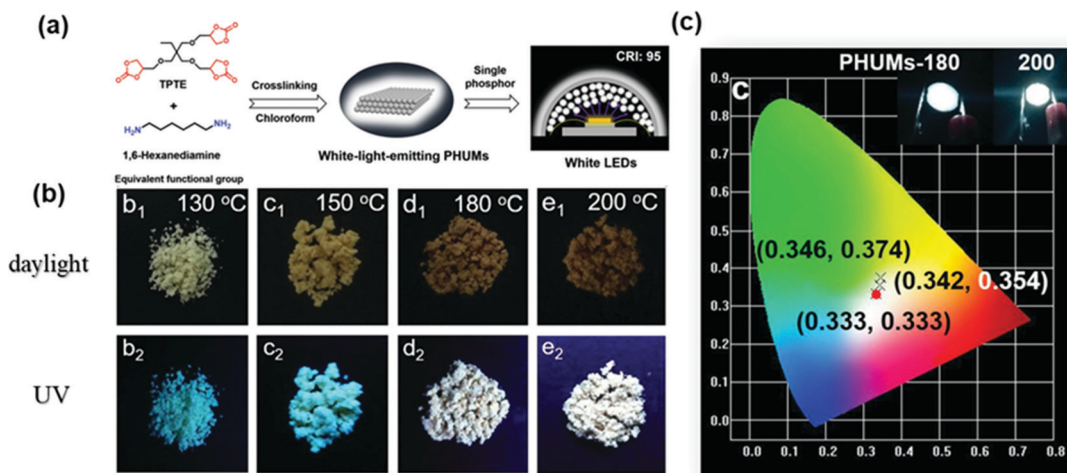


Fig. 21 (a) Preparation of poly(hydroxyurethane) microspheres (PHUMs) and their application in white LEDs. (b) Images of the PHUMs prepared at different temperatures taken under daylight and UV light (365 nm). (c) CIE chromaticity coordinates of the white LEDs. Reproduced with permission from ref. 56. Copyright 2020, Wiley-VCH.

temperature. As illustrated in Fig. 21(b), regular microspheres were prepared at 130, 150, 180, and 200 °C and were denoted as PHUMs-130, PHUMs-150, PHUMs-180, and PHUMs-200, respectively. As the synthesis temperature was increased, the fluorescence of the PHUMs emitted under 365 nm excitation gradually red shifted. Finally, the Commission International de L'Eclairage (CIE) coordinates of PHUMs-180 and PHUMs-200 were located at (0.342, 0.354) and (0.346, 0.374), respectively, which were close to that of pure white light (0.33, 0.33) [Fig. 21(c)], providing an ideal candidate for the facile fabrication of phosphor-converted white LEDs.

Bioimaging

Fluorescence has always been an important means for humans to observe life activities in organisms, such as cancer cell growth and inhibition, drug release and metabolism, protein status and function, *etc.* There have been several reports on using CTE materials for cell imaging, included polyamide,³⁸ polysaccharide,⁴³ polyurethane¹⁹ and so on. In 2019, Nie *et al.* reported a novel fluorescent polymer (HBPSi-CD) with rigid β -cyclodextrin attached to the end of the flexible polysiloxane chain of hyperbranched polysiloxane (HBPSi).⁴⁹ As shown in Fig. 22(a), the biocompatible HBPSi-CD not only lit up mouse fibroblast cells, but also possessed a high ibuprofen loading capacity (160 mg g⁻¹) and a superior pH-responsive drug-release performance. In another study, spiropolymers P1a2b were prepared, which showed CTE properties and strong fluorescence in cancer cells, resulting from strong interactions with the MDM2 protein [Fig. 22(b)]. By preventing the anti-apoptotic p53/MDM2 interaction, P1a2b triggered apoptosis in cancerous cells, while demonstrating good biocompatibility and non-toxicity in non-cancerous cells.⁵⁵ Due to the CTE nature of the protein itself, the aggregation state of the protein can also be judged by the fluorescence intensity that requires no chemical modification or labelling.⁴⁶ Fig. 22(c) illustrates the evolution of the intrinsic fluorescence of I59T lysozyme imaged using TCSPC-FLIM throughout the time course of the aggregation process. It is clear from these images that the number of fluorescent aggregates increases with time.

Detection of metal ions and small molecules

As CTE materials are rich in atoms with a high electro-negativity, they can often coordinate with metal ions, change their aggregation state, and then change the light-emitting state. Therefore, they can be used to detect metal ions specifically. The following two examples are of Fe³⁺ suppressing CTE emission⁴² [Fig. 23(a)] and Zn²⁺ promoting emission⁶⁰ [Fig. 23(b)].

There are also reports on the detection of small molecules, especially explosives.^{19,36,37,122} For example, the PAMAM dendrimer was successfully used for the detection of 2,4-dinitrotoluene (DNT) as reported by Ghosh and Koley.¹²² PAMAM acts as an electron-donating center in the presence of electron-deficient molecules such as DNT. The strong host-guest interaction holds the redox centers at a proximal distance, which causes accelerated electron-transfer kinetics for

the dendrimer-DNT redox couple to produce rapid quenching [Fig. 24].

Summary and perspective

NTIL materials with CTE properties are emerging as a new class of luminogens. In comparison with traditional π -conjugated systems, the clusterization of non-conventional luminogens with π and n electrons and subsequent TSC result in extended electron delocalization and conformation rigidification rationalizing the emission. As a result, its luminescence tends to be wavelength-dependent and concentration-dependent, and it is easy to produce room-temperature phosphorescence.

The research on CTE can be divided into two important directions. One is molecular design. CTE materials usually require abundant lone pairs of electrons in the systems. Functional groups rich in O, N, S, P, and Si, such as hydroxyl (-OH), ether (-O-), carboxylic acid (-COOH), ester (-COOR), anhydride (-COOCO-), amide (-NHCO-), amine (-NH₂), nitrile (-CN), pyridine (-C₅H₅N), thioamide (-NHCS-), sulfide (-S-), sulfonate (-SO₃H), sulfoxide (-SO), sulfone (-OSO-), phosphate (-PO₃-) and siloxane (-SiO), should be considered to be reasonably introduced into the system. In addition, there are some strategies that can be referred to: (1) the introduction of charges may enhance the TSC effect; (2) the introduction of halogen groups can change the luminescence state of its room-temperature phosphorescence; (3) the design of donor-acceptor structures or interaction with the conjugated luminescence system in the way of energy transfer may produce more abundant luminescence phenomena. On the other hand, it is also important to control the aggregation state of the CTE materials. People have generally realized that both a denser aggregation state and a larger aggregate size can improve the efficiency of CTE luminescence. Organic-inorganic hybridization, including the coordination of metal ions and the enrichment of clusteroluminogens on the surface of metal clusters, can often meet the dual needs of molecular structure and aggregation state at the same time. However, more refined structural adjustments and in-depth theoretical and experimental investigations are still needed to gain insight into this phenomenon.

CTE materials can significantly reduce the tedious organic synthesis, which extends important potential for practical applications. In addition, the unique luminescence principles allow CTE materials to display superior properties in many fields such as multi-color luminescence, room-temperature phosphorescence, bioimaging, optical sensing, *etc.* However, there is still a long way to go for CTE to play a dominating role in practical applications. Some important issues should be tackled, such as (1) the broad emission due to the presence of multiple emission species, (2) most of the emission is limited to 400–500 nm, and the fluorescence efficiency is low, (3) it is hard to produce circularly polarized light in a pure organic CTE system due to the complexity and unpredictability of the formed conjugated structure.

In order to achieve fine control of the aggregation state, partially solve the defects of CTE materials, and further expand

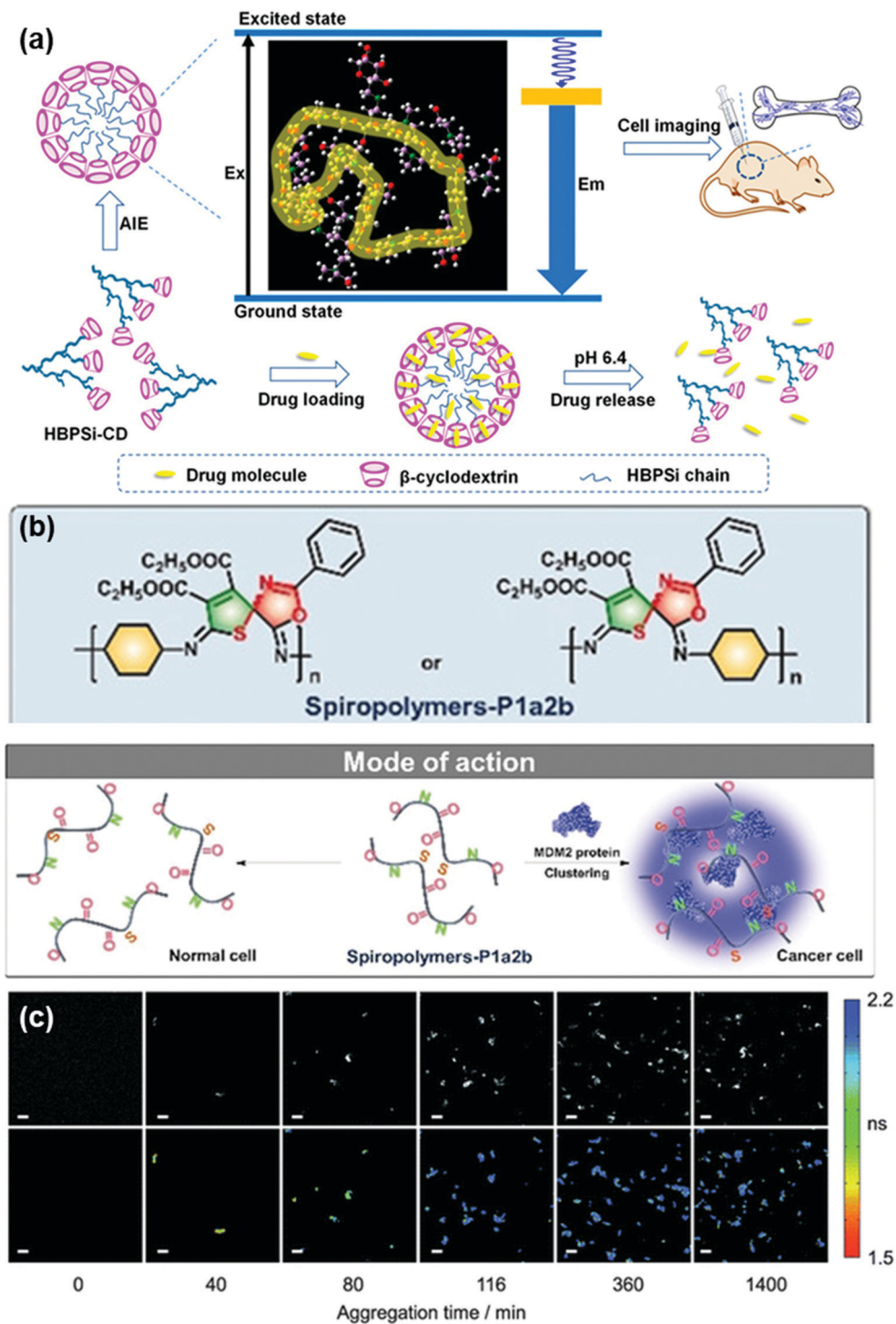


Fig. 22 (a) Biological applications of HBPSi-CD. (b) The structure of P1a2b and plausible MDM2-sensing mode of action. (c) Fluorescence intensity (upper panel) and lifetime (lower panel) of the aggregates present at various time points during the aggregation process (0, 40, 80, 116, 360 and 1400 min). Scale bars, 20 μm . Figures reproduced with permission from (a) ref. 49. Copyright 2019, American Chemical Society; (b) ref. 55. Copyright 2020, Wiley-VCH and (c) ref. 46. Copyright 2013, Royal Society of Chemistry.

the perspective of CTE research, we envision generating CTE in supramolecular self-assembled structures as the supramolecular assembled CTE system may have the following characteristics:

(I) The introduction of sufficient non-covalent supramolecular interactions would compensate for the concentration

effect and achieve the CTE effect at low concentrations [Fig. 25(a)].

(II) The self-assembled CTE systems with well-defined sizes and structures would provide unified spatial conjugation, so the luminescence characteristics that depend on excitation

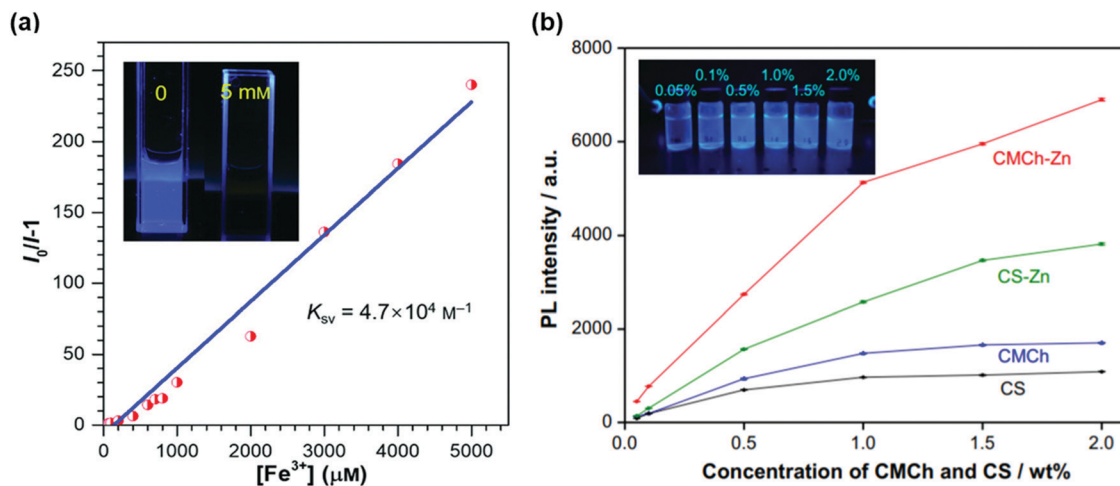


Fig. 23 (a) Stern–Volmer plots of the net increase in peak intensity ($I_0/I - 1$) at 396 nm against $[\text{Fe}^{3+}]$ in aqueous PEG solutions. The inset images are the solutions with $[\text{Fe}^{3+}]$ of 0 and 5 mM taken under 312 nm UV light. (b) Comparison of PL intensity for different concentrations of CMCh and CS solutions before and after mixing with 0.005 M of Zn^{2+} at pH = 6.4. Figures reproduced with permission from (a) ref. 42. Copyright 2018, Wiley-VCH and (b) ref. 60. Copyright 2020, Elsevier B.V.

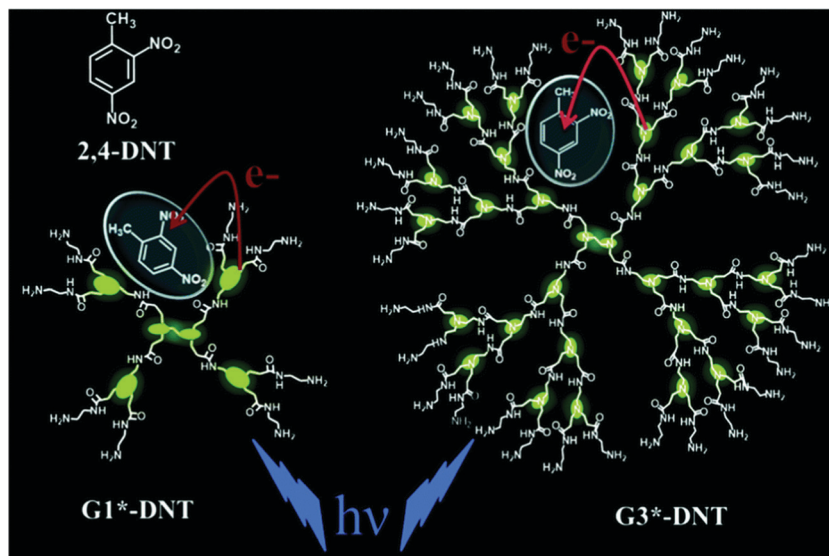


Fig. 24 Schematic representations of PAMAM dendrimer–DNT complexes. Reproduced with permission from ref. 122. Copyright 2016, Royal Society of Chemistry.

will disappear and the luminescence purity will be improved [Fig. 25(b)].

(III) Environmental stimuli that are efficient in modifying the strength of different supramolecular forces and further adjusting the self-assembled structures, such as temperature, pH, salts, light, and solvents, could be applicable in fine-tuning the color of CTE, making it possible to generate full-spectrum emission, as well as stimuli-responsive CTE [Fig. 25(c)].

(IV) Chiral self-assembly of CTE systems is a possible approach for generating circularly polarized luminescence that has great potential to replace conventional CPL materials [Fig. 25(d)]. A crucial requirement for the occurrence of CPL is

alignment of the chromophores in a chiral environment.^{123–125} There have been reports on CPL from clusters of metal atoms.^{126–130} However, aligning the clusteroluminogens in a purely organic CTE system remains an insurmountable challenge as the clustering states of the clusteroluminogens are always heterogeneous. If the clusteroluminogens are aligned (oriented alignment) properly, the supramolecular chirality formed may bring high chiral dissymmetry.^{131–133}

Currently, there is still no research focusing on self-assembled purely organic CTE materials. One of the main reasons is the lack of self-assembling ability of organic CTE molecules. Most organic CTE molecules contain a large number of polar

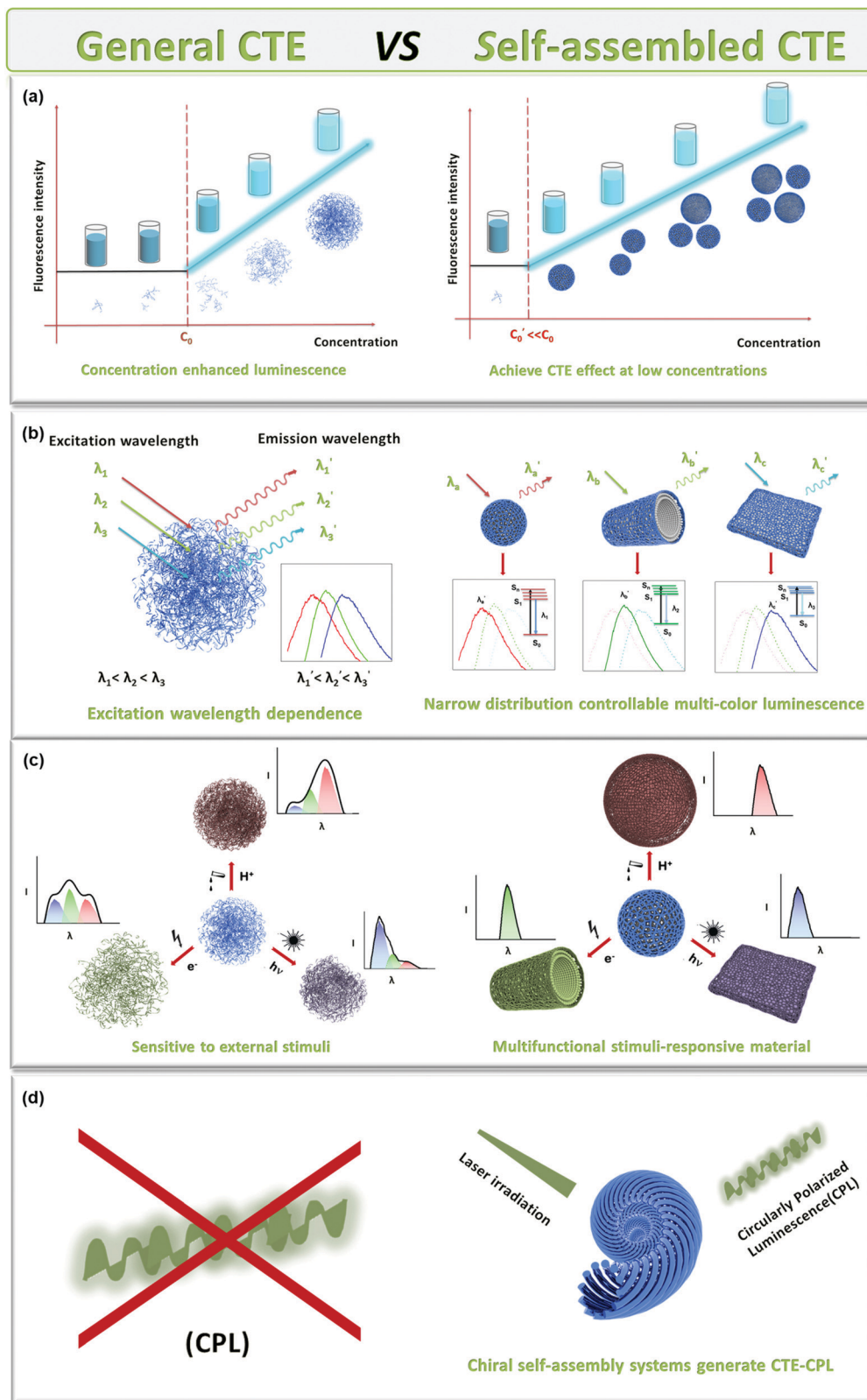


Fig. 25 Advantages of self-assembled CTE systems compared with general CTE systems.

groups, such that they usually interact strongly with the solvent. It is appealing to develop appropriate methods to drive the formation

of well-defined supramolecular assemblies of CTE molecules, and we look forward to steering towards this goal in the near future.

Conflicts of interest

There are no conflicts to declare.

Acknowledgements

This work was financially supported by the National Natural Science Foundation of China (NSFC 91856120, 21633002).

References

- 1 R. Y. Tsien, The green fluorescent protein, *Annu. Rev. Biochem.*, 1998, **67**, 509–544.
- 2 M. Chalfie, Y. Tu, G. Euskirchen, W. W. Ward and D. C. Prasher, Green fluorescent protein as a marker for gene expression, *Science*, 1994, **263**, 802–805.
- 3 D. A. Tomalia, B. Klajnert-Maculewicz, K. A. M. Johnson, H. F. Brinkman, A. Janaszewska and D. M. Hedstrand, Non-traditional intrinsic luminescence: Inexplicable blue fluorescence observed for dendrimers, macromolecules and small molecular structures lacking traditional/conventional luminophores, *Prog. Polym. Sci.*, 2019, **90**, 35–117.
- 4 A. M. Halpern, The vapor state emission from a saturated amine, *Chem. Phys. Lett.*, 1970, **6**, 296–298.
- 5 B. Z. Tang, X. W. Zhan, G. Yu, P. P. S. Lee, Y. Q. Liu and D. B. Zhu, Efficient blue emission from siloles, *J. Mater. Chem.*, 2001, **11**, 2974–2978.
- 6 J. Luo, Z. Xie, J. W. Lam, L. Cheng, H. Chen, C. Qiu, H. S. Kwok, X. Zhan, Y. Liu, D. Zhu and B. Z. Tang, Aggregation-induced emission of 1-methyl-1,2,3,4,5-pentaphenylsilole, *Chem. Commun.*, 2001, 1740–1741, DOI: 10.1039/b105159h.
- 7 Y. Hong, J. W. Lam and B. Z. Tang, Aggregation-induced emission, *Chem. Soc. Rev.*, 2011, **40**, 5361–5388.
- 8 Y. C. Chen, J. W. Y. Lam, R. T. K. Kwok, B. Liu and B. Z. Tang, Aggregation-induced emission: Fundamental understanding and future developments, *Mater. Horiz.*, 2019, **6**, 428–433.
- 9 Q. Peng, Y. Yi, Z. Shuai and J. Shao, Toward quantitative prediction of molecular fluorescence quantum efficiency: Role of duschinsky rotation, *J. Am. Chem. Soc.*, 2007, **129**, 9333–9339.
- 10 T. Zhang, Y. Jiang, Y. Niu, D. Wang, Q. Peng and Z. Shuai, Aggregation effects on the optical emission of 1,1,2,3,4,5-hexaphenylsilole (HPS): A QM/MM study, *J. Phys. Chem. A*, 2014, **118**, 9094–9104.
- 11 J. Mei, Y. Hong, J. W. Lam, A. Qin, Y. Tang and B. Z. Tang, Aggregation-induced emission: The whole is more brilliant than the parts, *Adv. Mater.*, 2014, **26**, 5429–5479.
- 12 J. Mei, N. L. Leung, R. T. Kwok, J. W. Lam and B. Z. Tang, Aggregation-induced emission: together we shine, united we soar!, *Chem. Rev.*, 2015, **115**, 11718–11940.
- 13 C. Wang and Z. Li, Molecular conformation and packing: Their critical roles in the emission performance of mechanochromic fluorescence materials, *Mater. Chem. Front.*, 2017, **1**, 2174–2194.
- 14 C. M. Xing, J. W. Y. Lam, A. Qin, Y. Dong, M. Haussler, W. T. Yang and B. Z. Tang, Unique photoluminescence from nonconjugated alternating copolymer poly[(maleic anhydride)-*alt*-(vinyl acetate)], *Polym. Mater. Sci. Eng.*, 2007, **96**, 418–419.
- 15 Y. Y. Gong, Y. Q. Tan, J. Mei, Y. R. Zhang, W. Z. Yuan, Y. M. Zhang, J. Z. Sun and B. Z. Tang, Room temperature phosphorescence from natural products: Crystallization matters, *Sci. China: Chem.*, 2013, **56**, 1178–1182.
- 16 Q. Zhou, B. Cao, C. Zhu, S. Xu, Y. Gong, W. Z. Yuan and Y. Zhang, Clustering-triggered emission of nonconjugated polyacrylonitrile, *Small*, 2016, **12**, 6586–6592.
- 17 X. H. Chen, Y. Z. Wang, Y. M. Zhang and W. Z. Yuan, Clustering-triggered emission of nonconventional luminophores, *Prog. Chem.*, 2019, **31**, 1560–1575.
- 18 Z. H. Zhao, X. H. Chen, Q. Wang, T. J. Yang, Y. M. Zhang and W. Z. Yuan, Sulphur-containing nonaromatic polymers: Clustering-triggered emission and luminescence regulation by oxidation, *Polym. Chem.*, 2019, **10**, 3639–3646.
- 19 X. H. Chen, X. D. Liu, J. L. Lei, L. Xu, Z. H. Zhao, F. Kausar, X. Y. Xie, X. Y. Zhu, Y. M. Zhang and W. Z. Yuan, Synthesis, clustering-triggered emission, explosive detection and cell imaging of nonaromatic polyurethanes, *Mol. Syst. Des. Eng.*, 2018, **3**, 364–375.
- 20 X. H. Chen, W. J. Luo, H. L. Ma, Q. Peng, W. Z. Yuan and Y. M. Zhang, Prevalent intrinsic emission from nonaromatic amino acids and poly(amino acids), *Sci. China: Chem.*, 2018, **61**, 351–359.
- 21 W. Z. Yuan and Y. M. Zhang, Nonconventional macromolecular luminogens with aggregation-induced emission characteristics, *J. Polym. Sci. Pol. Chem.*, 2017, **55**, 560–574.
- 22 H. K. Zhang, Z. Zhao, P. R. McGonigal, R. Q. Ye, S. J. Liu, J. W. Y. Lam, R. T. K. Kwok, W. Z. Yuan, J. P. Xie, A. L. Rogach and B. Z. Tang, Clusterization-triggered emission: uncommon luminescence from common materials, *Mater. Today*, 2020, **32**, 275–292.
- 23 O. Varnavski, R. G. Ispasoiu, L. Balogh, D. Tomalia and T. Goodson, Ultrafast time-resolved photoluminescence from novel metal-dendrimer nanocomposites, *J. Chem. Phys.*, 2001, **114**, 1962–1965.
- 24 D. Wang and T. Imae, Fluorescence emission from dendrimers and its pH dependence, *J. Am. Chem. Soc.*, 2004, **126**, 13204–13205.
- 25 W. I. Lee, Y. Bae and A. J. Bard, Strong blue photoluminescence and ECL from OH-terminated PAMAM dendrimers in the absence of gold nanoparticles, *J. Am. Chem. Soc.*, 2004, **126**, 8358–8359.
- 26 S. Y. Lin, T. H. Wu, Y. C. Jao, C. P. Liu, H. Y. Lin, L. W. Lo and C. S. Yang, Unraveling the photoluminescence puzzle of PAMAM dendrimers, *Chemistry*, 2011, **17**, 7158–7161.
- 27 R. B. Wang, W. Z. Yuan and X. Y. Zhu, Aggregation-induced emission of non-conjugated poly(amido amine)s: Discovering, luminescent mechanism understanding and bioapplication, *Chin. J. Polym. Sci.*, 2015, **33**, 680–687.
- 28 D. Wang, T. Imae and M. Miki, Fluorescence emission from PAMAM and PPI dendrimers, *J. Colloid Interface Sci.*, 2007, **306**, 222–227.

- 29 W. Yu, Y. Wu, J. Chen, X. Duan, X.-F. Jiang, X. Qiu and Y. Li, Sulfonated ethylenediamine–acetone–formaldehyde condensate: preparation, unconventional photoluminescence and aggregation enhanced emission, *RSC Adv.*, 2016, **6**, 51257–51263.
- 30 H. Lu, L. Feng, S. Li, J. Zhang, H. Lu and S. Feng, Unexpected strong blue photoluminescence produced from the aggregation of unconventional chromophores in novel siloxane–poly(amidoamine) dendrimers, *Macromolecules*, 2015, **48**, 476–482.
- 31 D. Pinotsi, L. Grisanti, P. Mahou, R. Gebauer, C. F. Kaminski, A. Hassanali and G. S. Kaminski, Schierle, Proton transfer and structure-specific fluorescence in hydrogen bond-rich protein structures, *J. Am. Chem. Soc.*, 2016, **138**, 3046–3057.
- 32 A. Shukla, S. Mukherjee, S. Sharma, V. Agrawal, K. V. Radha Kishan and P. Guptasarma, A novel UV laser-induced visible blue radiation from protein crystals and aggregates: Scattering artifacts or fluorescence transitions of peptide electrons delocalized through hydrogen bonding?, *Arch. Biochem. Biophys.*, 2004, **428**, 144–153.
- 33 C. L. Larson and S. A. Tucker, Intrinsic fluorescence of carboxylate-terminated polyamido amine dendrimers, *Appl. Spectrosc.*, 2001, **55**, 679–683.
- 34 G. M. Brown and H. A. Levy, Alpha-D-glucose: Precise determination of crystal and molecular structure by neutron-diffraction analysis, *Science*, 1965, **147**, 1038–1039.
- 35 Q. Wang, X. Dou, X. Chen, Z. Zhao, S. Wang, Y. Wang, K. Sui, Y. Tan, Y. Gong, Y. Zhang and W. Z. Yuan, Reevaluating protein photoluminescence: Remarkable visible luminescence upon concentration and insight into the emission mechanism, *Angew. Chem., Int. Ed.*, 2019, **58**, 12667–12673.
- 36 M. Li, X. Li, X. An, Z. Chen and H. Xiao, Clustering-triggered emission of carboxymethylated nanocellulose, *Front. Chem.*, 2019, **7**, 447.
- 37 L. L. Du, B. L. Jiang, X. H. Chen, Y. Z. Wang, L. M. Zou, Y. L. Liu, Y. Y. Gong, C. Wei and W. Z. Yuan, Clustering-triggered emission of cellulose and its derivatives, *Chin. J. Polym. Sci.*, 2019, **37**, 409–415.
- 38 Q. Zhou, Z. Y. Wang, X. Y. Dou, Y. Z. Wang, S. E. Liu, Y. M. Zhang and W. Z. Yuan, Emission mechanism understanding and tunable persistent room temperature phosphorescence of amorphous nonaromatic polymers, *Mater. Chem. Front.*, 2019, **3**, 257–264.
- 39 S. Wang, K. Gu, Z. Guo, C. Yan, T. Yang, Z. Chen, H. Tian and W. H. Zhu, Self-assembly of a monochromophore-based polymer enables unprecedented ratiometric tracing of hypoxia, *Adv. Mater.*, 2019, **31**, e1805735.
- 40 N. Gan, H. F. Shi, Z. F. An and W. Huang, Recent advances in polymer-based metal-free room-temperature phosphorescent materials, *Adv. Funct. Mater.*, 2018, **28**, 24.
- 41 X. H. Chen, Z. H. He, F. Kausar, G. Chen, Y. M. Zhang and W. Z. Yuan, Aggregation-induced dual emission and unusual luminescence beyond excimer emission of poly(ethylene terephthalate), *Macromolecules*, 2018, **51**, 9035–9042.
- 42 Y. Wang, X. Bin, X. Chen, S. Zheng, Y. Zhang and W. Z. Yuan, Emission and emissive mechanism of nonaromatic oxygen clusters, *Macromol. Rapid Commun.*, 2018, **39**, e1800528.
- 43 X. Dou, Q. Zhou, X. Chen, Y. Tan, X. He, P. Lu, K. Sui, B. Z. Tang, Y. Zhang and W. Z. Yuan, Clustering-triggered emission and persistent room temperature phosphorescence of sodium alginate, *Biomacromolecules*, 2018, **19**, 2014–2022.
- 44 W. Huang, H. X. Yan, S. Niu, Y. Q. Du and L. Y. Yuan, Unprecedented strong blue photoluminescence from hyperbranched polycarbonate: From its fluorescence mechanism to applications, *J. Polym. Sci. Pol. Chem.*, 2017, **55**, 3690–3696.
- 45 T. Yang, S. Dai, S. Yang, L. Chen, P. Liu, K. Dong, J. Zhou, Y. Chen, H. Pan, S. Zhang, J. Chen, K. Zhang, P. Wu and J. Xu, Interfacial clustering-triggered fluorescence-phosphorescence dual solvoluminescence of metal nanoclusters, *J. Phys. Chem. Lett.*, 2017, **8**, 3980–3985.
- 46 F. T. Chan, G. S. Kaminski Schierle, J. R. Kumita, C. W. Bertocini, C. M. Dobson and C. F. Kaminski, Protein amyloids develop an intrinsic fluorescence signature during aggregation, *Analyst*, 2013, **138**, 2156–2162.
- 47 X. Bin, W. J. Luo, W. Z. Yuan and Y. M. Zhang, Clustering-triggered emission of poly(*N*-hydroxysuccinimide methacrylate), *Acta. Chim. Sin.*, 2016, **74**, 935–941.
- 48 Y. Q. Du, T. Bai, F. Ding, H. X. Yan, Y. Zhao and W. X. Feng, The inherent blue luminescence from oligomeric siloxanes, *Polym. J.*, 2019, **51**, 869–882.
- 49 C. Shang, Y. X. Zhao, N. Wei, H. M. Zhuo, Y. M. Shao and H. L. Wang, Enhancing photoluminescence of nonconventional luminescent polymers by increasing chain flexibility, *Macromol. Chem. Phys.*, 2019, **220**, 7.
- 50 L. Bai, H. Yan, T. Bai, Y. Feng, Y. Zhao, Y. Ji, W. Feng, T. Lu and Y. Nie, High fluorescent hyperbranched polysiloxane containing beta-cyclodextrin for cell imaging and drug delivery, *Biomacromolecules*, 2019, **20**, 4230–4240.
- 51 S. Zheng, T. Hu, X. Bin, Y. Wang, Y. Yi, Y. Zhang and W. Z. Yuan, Clustering-triggered efficient room-temperature phosphorescence from nonconventional luminophores, *ChemPhysChem*, 2020, **21**, 36–42.
- 52 H. Wang, H. Shi, W. Ye, X. Yao, Q. Wang, C. Dong, W. Jia, H. Ma, S. Cai, K. Huang, L. Fu, Y. Zhang, J. Zhi, L. Gu, Y. Zhao, Z. An and W. Huang, Amorphous ionic polymers with color-tunable ultralong organic phosphorescence, *Angew. Chem., Int. Ed.*, 2019, **58**, 18776–18782.
- 53 Y. Q. Du, T. Bai, H. X. Yan, Y. Zhao, W. X. Feng and W. Q. Li, A simple and convenient route to synthesize novel hyperbranched poly(amine ester) with multicolored fluorescence, *Polymer*, 2019, **185**, 10.
- 54 C. Shang, Y. X. Zhao, J. Y. Long, Y. Ji and H. L. Wang, Orange-red and white-emitting nonconventional luminescent polymers containing cyclic acid anhydride and lactam groups, *J. Mater. Chem. C*, 2020, **8**, 1017–1024.
- 55 P. Liu, W. Fu, P. Verwilt, M. Won, J. Shin, Z. Cai, B. Tong, J. Shi, Y. Dong and J. S. Kim, MDM2-Associated clusterization-triggered emission and apoptosis induction effectuated by a theranostic spiropolymer, *Angew. Chem., Int. Ed.*, 2020, **59**, 8435–8439.

- 56 B. Liu, B. Chu, Y. L. Wang, Z. Chen and X. H. Zhang, Crosslinking-induced white light emission of poly(hydroxyurethane) microspheres for white LEDs, *Adv. Opt. Mater.*, 2020, **8**, 7.
- 57 S. Zheng, T. Zhu, Y. Wang, T. Yang and W. Z. Yuan, Accessing tunable afterglows from highly twisted nonaromatic organic AIEgens via effective through-space conjugation, *Angew. Chem., Int. Ed.*, 2020, **59**, 10018–10022.
- 58 Q. Zhou, T. Yang, Z. Zhong, F. Kausar, Z. Wang, Y. Zhang and W. Z. Yuan, A clustering-triggered emission strategy for tunable multicolor persistent phosphorescence, *Chem. Sci.*, 2020, **11**, 2926–2933.
- 59 S. Tao, S. Zhu, T. Feng, C. Zheng and B. Yang, Crosslink-enhanced emission effect on luminescence in polymers: Advances and perspectives, *Angew. Chem., Int. Ed.*, 2020, **59**, 9826–9840.
- 60 J. Huang, Y. L. Wang, X. D. Yu, Y. N. Zhou and L. Q. Chu, Enhanced fluorescence of carboxymethyl chitosan via metal ion complexation in both solution and hydrogel states, *Int. J. Biol. Macromol.*, 2020, **152**, 50–56.
- 61 M. M. Fang, J. Yang, X. Q. Xiang, Y. J. Xie, Y. Q. Dong, Q. Peng, Q. Q. Li and Z. Li, Unexpected room-temperature phosphorescence from a non-aromatic, low molecular weight, pure organic molecule through the intermolecular hydrogen bond, *Mater. Chem. Front.*, 2018, **2**, 2124–2129.
- 62 J. J. Yan, B. Zheng, D. H. Pan, R. L. Yang, Y. P. Xu, L. Z. Wang and M. Yang, Unexpected fluorescence from polymers containing dithio/amino-succinimides, *Polym. Chem.*, 2015, **6**, 6133–6139.
- 63 S. Bhattacharya, V. N. Rao, S. Sarkar and R. Shunmugam, Unusual emission from norbornene derived phosphonate molecule—a sensor for Fe(III) in aqueous environment, *Nanoscale*, 2012, **4**, 6962–6966.
- 64 L. Liu, H. K. Zhang, S. J. Liu, J. Z. Sun, X. H. Zhang and B. Z. Tang, Polymerization-induced emission, *Mater. Horiz.*, 2020, **7**, 987–998.
- 65 X. Miao, T. Liu, C. Zhang, X. Geng, Y. Meng and X. Li, Fluorescent aliphatic hyperbranched polyether: Chromophore-free and without any N and P atoms, *Phys. Chem. Chem. Phys.*, 2016, **18**, 4295–4299.
- 66 A. Pucci, R. Rausa and F. Ciardelli, Aggregation-induced luminescence of polyisobutene succinic anhydrides and imides, *Macromol. Chem. Phys.*, 2008, **209**, 900–906.
- 67 E. Zhao, J. W. Y. Lam, L. M. Meng, Y. Hong, H. Q. Deng, G. X. Bai, X. H. Huang, J. H. Hao and B. Z. Tang, Poly-[(maleic anhydride)-*alt*-(vinyl acetate)]: A pure oxygenic nonconjugated macromolecule with strong light emission and solvatochromic effect, *Macromolecules*, 2015, **48**, 64–71.
- 68 Q. Zhang, Q. Y. Mao, C. Shang, Y. N. Chen, X. Peng, H. W. Tan and H. L. Wang, Simple aliphatic oximes as nonconventional luminogens with aggregation-induced emission characteristics, *J. Mater. Chem. C*, 2017, **5**, 3699–3705.
- 69 F. Bacon and W. A. Wright, *Bacon the Advancement of Learning*, Clarendon Press, 1869.
- 70 W. Z. Li, X. Y. Wu, Z. J. Zhao, A. J. Qin, R. R. Hu and B. Z. Tang, Catalyst-Free, Atom-economic, multicomponent polymerizations of aromatic diynes, elemental sulfur, and aliphatic diamines toward luminescent polythioamides, *Macromolecules*, 2015, **48**, 7747–7754.
- 71 L. Cao, W. L. Yang, C. C. Wang and S. K. Fu, Synthesis and striking fluorescence properties of hyperbranched poly-(amido amine), *J. Macromol. Sci., Part A: Pure Appl. Chem.*, 2007, **44**, 417–424.
- 72 G. Jayamurugan, C. P. Umesh and N. Jayaraman, Inherent photoluminescence properties of poly(propyl ether imine) dendrimers, *Org. Lett.*, 2008, **10**, 9–12.
- 73 X. Pan, G. Wang, C. L. Lay, B. H. Tan, C. He and Y. Liu, Photoluminescence from amino-containing polymer in the presence of CO₂: Carbamate anion formed as a fluorophore, *Sci. Rep.*, 2013, **3**, 2763.
- 74 L. Pastor-Perez, Y. Chen, Z. Shen, A. Lahoz and S. E. Stiriba, Unprecedented blue intrinsic photoluminescence from hyperbranched and linear polyethylenimines: Polymer architectures and pH-effects, *Macromol. Rapid Commun.*, 2007, **28**, 1404–1409.
- 75 S. F. Shiau, T. Y. Juang, H. W. Chou and M. Liang, Synthesis and properties of new water-soluble aliphatic hyperbranched poly(amido acids) with high pH-dependent photoluminescence, *Polymer*, 2013, **54**, 623–630.
- 76 D. C. Wu, Y. Liu, C. B. He and S. H. Goh, Blue photoluminescence from hyperbranched poly(amino ester)s, *Macromolecules*, 2005, **38**, 9906–9909.
- 77 T. Liu, Y. Meng, X. C. Wang, H. Q. Wang and X. Y. Li, Unusual strong fluorescence of a hyperbranched phosphate: Discovery and explanations, *RSC Adv.*, 2013, **3**, 8269–8275.
- 78 M. G. Mohamed, K. C. Hsu, J. L. Hong and S. W. Kuo, Unexpected fluorescence from maleimide-containing polyhedral oligomeric silsesquioxanes: Nanoparticle and sequence distribution analyses of polystyrene-based alternating copolymers, *Polym. Chem.*, 2016, **7**, 135–145.
- 79 C. Liu, Q. Cui, J. Wang, Y. Liu and J. Chen, Autofluorescent micelles self-assembled from an AIE-active luminogen containing an intrinsic unconventional fluorophore, *Soft Matter*, 2016, **12**, 4295–4299.
- 80 J. Zheng, J. T. Petty and R. M. Dickson, High quantum yield blue emission from water-soluble Au₈ nanodots, *J. Am. Chem. Soc.*, 2003, **125**, 7780–7781.
- 81 Z. Luo, X. Yuan, Y. Yu, Q. Zhang, D. T. Leong, J. Y. Lee and J. Xie, From aggregation-induced emission of Au(I)-thiolate complexes to ultrabright Au(0)@Au(I)-thiolate core-shell nanoclusters, *J. Am. Chem. Soc.*, 2012, **134**, 16662–16670.
- 82 H. Cao, B. Li, X. Jiang, X. Zhu and X. Z. Kong, Fluorescent linear polyurea based on toluene diisocyanate: Easy preparation, broad emission and potential applications, *Chem. Eng. J.*, 2020, **399**, 125867.
- 83 Q. Zhou, J. Cui, T. J. Yang, C. L. Hu, Z. H. Zhong, Z. H. Sun, Y. Y. Gong, S. P. Pei and Y. M. Zhang, Intrinsic emission and tunable phosphorescence of perfluorosulfonate ionomers with evolved ionic clusters, *Sci. China: Chem.*, 2020, **63**, 833–840.
- 84 H. Lu, Z. Hu and S. Feng, Nonconventional luminescence enhanced by silicone-induced aggregation, *Chem. – Asian J.*, 2017, **12**, 1213–1217.

- 85 J. H. Zhou, L. W. Shi, C. Y. Zhang, H. Z. Li, M. B. Chen and W. M. Chen, Theoretical analysis of the formation driving force and decreased sensitivity for CL-20 cocrystals, *J. Mol. Struct.*, 2016, **1116**, 93–101.
- 86 X. B. Zhou, W. W. Luo, H. Nie, L. G. Xu, R. R. Hu, Z. J. Zhao, A. J. Qin and B. Z. Tang, Oligo(maleic anhydride)s: A platform for unveiling the mechanism of clusteroluminescence of non-aromatic polymers, *J. Mater. Chem. C*, 2017, **5**, 4775–4779.
- 87 H. Zhang, L. Du, L. Wang, J. Liu, Q. Wan, R. T. K. Kwok, J. W. Y. Lam, D. L. Phillips and B. Z. Tang, Visualization and manipulation of molecular motion in the solid state through photoinduced clusteroluminescence, *J. Phys. Chem. Lett.*, 2019, **10**, 7077–7085.
- 88 R. Kabe, N. Notsuka, K. Yoshida and C. Adachi, Afterglow organic light-emitting diode, *Adv. Mater.*, 2016, **28**, 655–660.
- 89 T. L. Chiu, H. J. Chen, Y. H. Hsieh, J. J. Huang and M. K. Leung, High-efficiency blue phosphorescence organic light-emitting diode with ambipolar carbazole-triazole host, *J. Phys. Chem. C*, 2015, **119**, 16846–16852.
- 90 W. Song and J. Y. Lee, Degradation mechanism and lifetime improvement strategy for blue phosphorescent organic light-emitting diodes, *Adv. Opt. Mater.*, 2017, **5**, 1600901.
- 91 Z. Yu, Y. Wu, L. Xiao, J. Chen, Q. Liao, J. Yao and H. Fu, Organic phosphorescence nanowire lasers, *J. Am. Chem. Soc.*, 2017, **139**, 6376–6381.
- 92 R. Gao, X. Y. Fang and D. P. Yan, Direct white-light emitting room-temperature-phosphorescence thin films with tunable two-color polarized emission through orientational hydrogen-bonding layer-by-layer assembly, *J. Mater. Chem. C*, 2018, **6**, 4444–4449.
- 93 Z. An, C. Zheng, Y. Tao, R. Chen, H. Shi, T. Chen, Z. Wang, H. Li, R. Deng, X. Liu and W. Huang, Stabilizing triplet excited states for ultralong organic phosphorescence, *Nat. Mater.*, 2015, **14**, 685–690.
- 94 S. Cai, H. Shi, J. Li, L. Gu, Y. Ni, Z. Cheng, S. Wang, W. W. Xiong, L. Li, Z. An and W. Huang, Visible-light-excited ultralong organic phosphorescence by manipulating intermolecular interactions, *Adv. Mater.*, 2017, **29**, 1701244.
- 95 Y. Su, S. Z. F. Phua, Y. Li, X. Zhou, D. Jana, G. Liu, W. Q. Lim, W. K. Ong, C. Yang and Y. Zhao, Ultralong room temperature phosphorescence from amorphous organic materials toward confidential information encryption and decryption, *Sci. Adv.*, 2018, **4**, eaas9732.
- 96 D. Lee, O. Bolton, B. C. Kim, J. H. Youk, S. Takayama and J. Kim, Room temperature phosphorescence of metal-free organic materials in amorphous polymer matrices, *J. Am. Chem. Soc.*, 2013, **135**, 6325–6329.
- 97 M. S. Kwon, D. Lee, S. Seo, J. Jung and J. Kim, Tailoring intermolecular interactions for efficient room-temperature phosphorescence from purely organic materials in amorphous polymer matrices, *Angew. Chem., Int. Ed.*, 2014, **53**, 11177–11181.
- 98 Y. Yu, M. S. Kwon, J. Jung, Y. Zeng, M. Kim, K. Chung, J. Gierschner, J. H. Youk, S. M. Borisov and J. Kim, Room-temperature-phosphorescence-based dissolved oxygen detection by core-shell polymer nanoparticles containing metal-free organic phosphors, *Angew. Chem., Int. Ed.*, 2017, **56**, 16207–16211.
- 99 X. Chen, C. Xu, T. Wang, C. Zhou, J. Du, Z. Wang, H. Xu, T. Xie, G. Bi, J. Jiang, X. Zhang, J. N. Demas, C. O. Trindle, Y. Luo and G. Zhang, Versatile Room-temperature-phosphorescent materials prepared from N-substituted naphthalimides: Emission enhancement and chemical conjugation, *Angew. Chem., Int. Ed.*, 2016, **55**, 9872–9876.
- 100 S. M. A. Fatemina, Z. Mao, S. Xu, Z. Yang, Z. Chi and B. Liu, Organic nanocrystals with bright red persistent room-temperature phosphorescence for biological applications, *Angew. Chem., Int. Ed.*, 2017, **56**, 12160–12164.
- 101 A. Nicol, R. T. K. Kwok, C. Chen, W. Zhao, M. Chen, J. Qu and B. Z. Tang, Ultrafast delivery of aggregation-induced emission nanoparticles and pure organic phosphorescent nanocrystals by saponin encapsulation, *J. Am. Chem. Soc.*, 2017, **139**, 14792–14799.
- 102 X. Zhen, Y. Tao, Z. An, P. Chen, C. Xu, R. Chen, W. Huang and K. Pu, Ultralong phosphorescence of water-soluble organic nanoparticles for *in vivo* afterglow imaging, *Adv. Mater.*, 2017, **29**, 1606665.
- 103 J. Yang, X. Zhen, B. Wang, X. Gao, Z. Ren, J. Wang, Y. Xie, J. Li, Q. Peng, K. Pu and Z. Li, The influence of the molecular packing on the room temperature phosphorescence of purely organic luminogens, *Nat. Commun.*, 2018, **9**, 840.
- 104 Kenry, C. Chen and B. Liu, Enhancing the performance of pure organic room-temperature phosphorescent luminophores, *Nat. Commun.*, 2019, **10**, 2111.
- 105 F. W. J. Teale, Principles of fluorescence spectroscopy – Lakowicz, Jr, *Nature*, 1984, **307**, 486.
- 106 A. H. Maki and J. A. Zuclich, Protein triplet states, in *Triplet States I. Topics in Current Chemistry*, ed. A. Devaquet, W. G. Dauben, G. Lodder, J. Ipaktschi, A. H. Maki, J. A. Zuclich, 1975, vol. 54.
- 107 M. L. Saviotti and W. C. Galley, Room temperature phosphorescence and the dynamic aspects of protein structure, *Proc. Natl. Acad. Sci. U. S. A.*, 1974, **71**, 4154–4158.
- 108 D. Jia, L. Cao, D. Wang, X. Guo, H. Liang, F. Zhao, Y. Gu and D. Wang, Uncovering a broad class of fluorescent amine-containing compounds by heat treatment, *Chem. Commun.*, 2014, **50**, 11488–11491.
- 109 C. Shang, N. Wei, H. M. Zhuo, Y. M. Shao, Q. Zhang, Z. X. Zhang and H. L. Wang, Highly emissive poly(maleic anhydride-*alt*-vinyl pyrrolidone) with molecular weight-dependent and excitation-dependent fluorescence, *J. Mater. Chem. C*, 2017, **5**, 8082–8090.
- 110 Z. Guo, Y. Ru, W. Song, Z. Liu, X. Zhang and J. Qiao, Water-soluble polymers with strong photoluminescence through an eco-friendly and low-cost route, *Macromol. Rapid Commun.*, 2017, **38**, 1700099.
- 111 X. H. Wu, P. Luo, Z. Wei, Y. Y. Li, R. W. Huang, X. Y. Dong, K. Li, S. Q. Zang and B. Z. Tang, Guest-triggered aggregation-induced emission in silver chalcogenolate cluster metal-organic frameworks, *Adv. Sci.*, 2019, **6**, 1801304.

- 112 R. W. Huang, Y. S. Wei, X. Y. Dong, X. H. Wu, C. X. Du, S. Q. Zang and T. C. W. Mak, Hypersensitive dual-function luminescence switching of a silver-chalcogenolate cluster-based metal-organic framework, *Nat. Chem.*, 2017, **9**, 689–697.
- 113 X. Kang and M. Z. Zhu, Intra-cluster growth meets inter-cluster assembly: The molecular and supramolecular chemistry of atomically precise nanoclusters, *Coord. Chem. Rev.*, 2019, **394**, 1–38.
- 114 H. Liu, X. Gao, X. Zhuang, C. Tian, Z. Wang, Y. Li and A. L. Rogach, A specific electrochemiluminescence sensor for selective and ultra-sensitive mercury(II) detection based on dithiothreitol functionalized copper nanocluster/carbon nitride nanocomposites, *Analyst*, 2019, **144**, 4425–4431.
- 115 Z. G. Wang, Y. E. Shi, X. M. Yang, Y. Xiong, Y. X. Li, B. K. Chen, W. F. Lai and A. L. Rogach, Water-soluble biocompatible copolymer hypromellose grafted chitosan able to load exogenous agents and copper nanoclusters with aggregation-induced emission, *Adv. Funct. Mater.*, 2018, **28**, 1802848.
- 116 X. Yan, P. Wei, Y. Liu, M. Wang, C. Chen, J. Zhao, G. Li, M. L. Saha, Z. Zhou, Z. An, X. Li and P. J. Stang, Endo- and exo-functionalized tetraphenylethylene M12L24 nanospheres: fluorescence emission inside a confined space, *J. Am. Chem. Soc.*, 2019, **141**, 9673–9679.
- 117 M. Sugiuchi, J. Maeba, N. Okubo, M. Iwamura, K. Nozaki and K. Konishi, Aggregation-induced fluorescence-to-phosphorescence switching of molecular gold clusters, *J. Am. Chem. Soc.*, 2017, **139**, 17731–17734.
- 118 Z. Wang, B. Chen, A. S. Sussha, W. Wang, C. J. Reckmeier, R. Chen, H. Zhong and A. L. Rogach, All-copper nanocluster based down-conversion white light-emitting devices, *Adv. Sci.*, 2016, **3**, 1600182.
- 119 T. Q. Yang, S. Dai, H. Tan, Y. X. Zong, Y. Y. Liu, J. Q. Chen, K. Zhang, P. Wu, S. J. Zhang, J. H. Xu and Y. Tian, Mechanism of photoluminescence in Ag nanoclusters: metal-centered emission versus synergistic effect in ligand-centered emission, *J. Phys. Chem. C*, 2019, **123**, 18638–18645.
- 120 J. S. Mohanty, K. Chaudhari, C. Sudhakar and T. Pradeep, Metal-ion-induced luminescence enhancement in protein protected gold clusters, *J. Phys. Chem. C*, 2019, **123**, 28969–28976.
- 121 B. P. Jiang, Y. X. Yu, X. L. Guo, Z. Y. Ding, B. Zhou, H. Liang and X. C. Shen, White-emitting carbon dots with long alkyl-chain structure: Effective inhibition of aggregation caused quenching effect for label-free imaging of latent fingerprint, *Carbon*, 2018, **128**, 12–20.
- 122 S. Koley and S. Ghosh, The study of electron transfer reactions in a dendrimeric assembly: Proper utilization of dendrimer fluorescence, *Phys. Chem. Chem. Phys.*, 2016, **18**, 24830–24834.
- 123 J. Kumar, T. Nakashima and T. Kawai, Circularly polarized luminescence in chiral molecules and supramolecular assemblies, *J. Phys. Chem. Lett.*, 2015, **6**, 3445–3452.
- 124 H. Kubo, T. Hirose, T. Nakashima, T. Kawai, J. Y. Hasegawa and K. Matsuda, Tuning transition electric and magnetic dipole moments: [7]Helicenes showing intense circularly polarized luminescence, *J. Phys. Chem. Lett.*, 2021, **12**, 686–695.
- 125 Y. Kono, K. Nakabayashi, S. Kitamura, M. Shizuma, M. Fujiki and Y. Imai, Can chiral P(III) coordinate Eu(III)? Unexpected solvent dependent circularly polarised luminescence of BINAP and Eu(III)(hfa)₃ in chloroform and acetone, *RSC Adv.*, 2016, **6**, 40219–40224.
- 126 M. M. Zhang, X. Y. Dong, Z. Y. Wang, H. Y. Li, S. J. Li, X. Zhao and S. Q. Zang, AIE triggers the circularly polarized luminescence of atomically precise enantiomeric copper(I) alkynyl clusters, *Angew. Chem., Int. Ed.*, 2020, **59**, 10052–10058.
- 127 L. Yao, G. Niu, J. Li, L. Gao, X. Luo, B. Xia, Y. Liu, P. Du, D. Li, C. Chen, Y. Zheng, Z. Xiao and J. Tang, Circularly polarized luminescence from chiral tetranuclear copper(I) iodide Clusters, *J. Phys. Chem. Lett.*, 2020, **11**, 1255–1260.
- 128 H. Wu, X. He, B. Yang, C. C. Li and L. Zhao, Assembly-induced strong circularly polarized luminescence of spirocyclic chiral silver(I) clusters, *Angew. Chem., Int. Ed.*, 2021, **60**, 1535–1539.
- 129 Z. Han, X. L. Zhao, P. Peng, S. Li, C. Zhang, M. Cao, K. Li, Z. Y. Wang and S. Q. Zang, Intercluster aurophilicity-driven aggregation lighting circularly polarized luminescence of chiral gold clusters, *Nano Res.*, 2020, **13**, 3248–3252.
- 130 X. Y. Wang, J. Zhang, J. Yin, S. H. Liu and B. Z. Tang, More is better: Aggregation induced luminescence and exceptional chirality and circularly polarized luminescence of chiral gold clusters, *Mater. Chem. Front.*, 2021, **5**, 368–374.
- 131 T. Zhao, J. Han, X. Jin, Y. Liu, M. Liu and P. Duan, Enhanced circularly polarized luminescence from reorganized chiral emitters on the skeleton of a zeolitic imidazolate framework, *Angew. Chem., Int. Ed.*, 2019, **58**, 4978–4982.
- 132 J. Kumar, T. Nakashima, H. Tsumatori and T. Kawai, Circularly polarized luminescence in chiral aggregates: Dependence of morphology on luminescence dissymmetry, *J. Phys. Chem. Lett.*, 2014, **5**, 316–321.
- 133 R. Tempelaar, A. Stradomska, J. Knoester and F. C. Spano, Circularly polarized luminescence as a probe for long-range interactions in molecular aggregates, *J. Phys. Chem. B*, 2011, **115**, 10592–10603.